BcXYG1, a Secreted Xyloglucanase from *Botrytis cinerea*, Triggers Both Cell Death and Plant Immune Responses[1]

Wenjun Zhu,[a,b] Mordechi Ronen,[a] Yonatan Gur,[a] Anna Minz-Dub,[a] Gal Masrati,[c] Nir Ben-Tal,[c] Alon Savidor,[d] Itai Sharon,[a] Elad Eizner,[a,e] Oliver Valerius,[f] Gerhard H. Braus,[f] Kyle Bowler,[g] Maor Bar-Peled,[g] and Amir Sharon[a,2]

[a]Department of Molecular Biology and Ecology of Plants, Faculty of Life Sciences, Tel Aviv University, Tel Aviv 69978, Israel
[b]College of Biology and Pharmaceutical Engineering, Wuhan Polytechnic University, Wuhan 430023, People's Republic of China
[c]Department of Biochemistry and Molecular Biology, Faculty of Life Sciences, Tel Aviv University, Tel Aviv 69978, Israel
[d]Nancy and Stephen Grand Israel National Center for Personalized Medicine, Weizmann Institute of Science, Rehovot 76100, Israel
[e]Department of Physical Electronics, Fleischman Faculty of Engineering, Tel Aviv University, Tel Aviv 69978, Israel
[f]Complex Carbohydrate Research Center, Department of Plant Biology, University of Georgia, Athens, Georgia 30602-4712
[g]Department of Molecular Microbiology and Genetics and Göttingen Center for Molecular Biosciences, Georg-August-Universität, Goettingen, 37073 Germany

ORCID IDs: 0000-0002-9026-7221 (W.Z.); 0000-0003-1322-5762 (G.M.); 0000-0001-8884-6948 (A.Sa.); 0000-0002-3117-5626 (G.H.B.); 0000-0001-5375-0356 (K.B.); 0000-0002-6885-696X (M.B.-P.); 0000-0002-6045-9169 (A.Sh.).

In search of *Botrytis cinerea* cell death-inducing proteins, we found a xyloglucanase (BcXYG1) that induced strong necrosis and a resistance response in dicot plants. Expression of the *BcXYG1* gene was strongly induced during the first 12 h post inoculation, and analysis of disease dynamics using PathTrack showed that a *B. cinerea* strain overexpressing *BcXYG1* produced early local necrosis, supporting a role of BcXYG1 as an early cell death-inducing factor. The xyloglucanase activity of BcXYG1 was not necessary for the induction of necrosis and plant resistance, as a mutant of BcXYG1 lacking the xyloglucanase enzymatic activity retained both functions. Residues in two exposed loops on the surface of BcXYG1 were found to be necessary for the induction of cell death but not to induce plant resistance. Further analyses showed that BcXYG1 is apoplastic and possibly interacts with the proteins of the plant cell membrane and also that the BcXYG1 cell death-promoting signal is mediated by the leucine-rich repeat receptor-like kinases BAK1 and SOBIR1. Our findings support the role of cell death-inducing proteins in establishing the infection of necrotrophic pathogens and highlight the recognition of fungal apoplastic proteins by the plant immune system as an important mechanism of resistance against this class of pathogens.

Botrytis cinerea is a wide-host-range fungal pathogen, causing gray mold and rot diseases in a large number of agriculturally important crops, and it has been used as a model system to study pathogenicity in necrotrophic plant pathogens. The *B. cinerea* infection process includes two typical stages: an early stage characterized by local lesions followed by a late stage of fast-spreading lesions (Williamson et al., 2007). Recent studies of disease dynamics conducted with the aid of the PathTrack system led to the discovery of a third, intermediate stage, between the transition from local infection to lesion spreading (Eizner et al., 2017). Further analysis using this system revealed that differences in disease progression between the wild type and pathogenicity mutants were largely in parameters of the intermediate stage, highlighting it as the phase during which the fungus is most significantly exposed and affected by the plant defense. The initial phase was much less affected by fungal mutations or by external conditions, suggesting that it depends primarily on the ability of the fungus to form local necrosis. This result is in line with previous work showing that, toward the end of the early phase (about 36 h post infection [hpi]) and the beginning of the late stage (about 48 hpi), the fungus undergoes massive cell death, which is induced by the plant defense (Shlezinger et al., 2011). A working model derived from these findings proposed that, during the early infection phase, the fungus forms local necrosis without invading the host tissue. The model also predicts the early secretion of cell death-inducing factors and the fast formation of small spots of dead tissue, in which the fungus can establish itself and use as foci for growth in the following stages (Shlezinger et al., 2011).

A relatively small number of effectors have been described in host-specific and broad-host-range necrotrophic

pathogens, compared with the wealth of information and the large number of effectors described in biotrophic and hemibiotrophic fungal pathogens. For example, victorin from the oat (*Avena sativa*) pathogen *Cochliobolus victoriae* triggers hypersensitive response-like resistance in Arabidopsis (*Arabidopsis thaliana*), thereby facilitating the disease of necrotrophic pathogens (Lorang et al., 2007, 2012). *Parastagonospora nodorum* and *Pyrenophora tritici-repentis*, two host-specific wheat (*Triticum aestivum*) pathogens, secrete multiple effectors that induce severe necrosis and confer disease susceptibility in wheat genotypes with the specific corresponding sensitivity genes (Oliver et al., 2012; Gao et al., 2015; Shi et al., 2015). Effectors described in broad-host-range necrotrophic fungi are classified primarily as necrosis-inducing proteins (NIPs). Proteins in this category can induce necrosis in a wide range of dicot plants, and in a few cases, they were found to be important for infection (Oliver and Solomon, 2010; Frías et al., 2011; González et al., 2016). Main groups of NIPs are cerato platanins and the necrosis- and ethylene-inducing proteins (NEP and NEP-like [NLP]). Recent studies showed that some NIPs are recognized by the plant immune system, leading to pathogen-associated molecular pattern-triggered immunity (PTI). For example, nlp20, a conserved 20-amino acid fragment found in most NLPs, interacts with the Arabidopsis Leu-rich repeat (LRR) receptor protein RLP23, and the resulting immunity signal is transmitted via the RLP23-SOBIR1-BAK1 complex (Albert et al., 2015).

Cell wall-degrading enzymes (CWDEs) play a central role in diseases caused by necrotrophic pathogens by the maceration of host tissues at late stages of the disease. These enzymes hydrolyze the glycoside bond between two or more carbohydrates or between a carbohydrate and a noncarbohydrate residue, thereby reducing complex sugar polymers to simple sugars (Cantarel et al., 2009; Kubicek et al., 2014). Some CWDEs activate the plant immune response, either directly or through the release of cell wall elicitors (Poinssot et al., 2003; Zhang et al., 2014b; Benedetti et al., 2015; Ma et al., 2015; Wu et al., 2016), and also may induce necrosis when injected to plant tissues (Noda et al., 2010; Zhang et al., 2014b, 2015; Ma et al., 2015). In certain cases, this necrosis-inducing activity was found to be unrelated to the enzymatic activity, thus defining another class of NIPs. For example, Xyn11A, a *B. cinerea* glycosyl hydrolase family 11 xylanase, induces cell death in plant leaves independent of the xylanase activity and is necessary for the full virulence of *B. cinerea* (Brito et al., 2006; Noda et al., 2010). The *Trichoderma viride* ethylene-inducing xylanase, another glycosyl hydrolase family 11 xylanase, induces necrosis in tobacco (*Nicotiana benthamiana*) and tomato (*Solanum lycopersicum*) leaves independent of the enzymatic activity (Furman-Matarasso et al., 1999). XEG1 produced by the soybean (*Glycine max*) pathogen *Phytophthora sojae* triggers cell death and plant defense responses in a BAK1-dependent manner and independent of its xyloglucanase activity (Ma et al., 2015).

Recent findings have demonstrated that the plant apoplast is most likely a battleground where a variety of plant-pathogen interactions occur and determine the outcome of pathogen infections (De Wit, 2016; Du et al., 2016). Accordingly, and based on our working model (Shlezinger et al., 2011), we anticipate the secretion of NIPs to the plant apoplast by *B. cinerea* in early infection stages. In search of such cell death-inducing virulence proteins, we conducted a proteomic analysis of the *B. cinerea* secretome that was collected from infected leaves and screened candidates for necrosis-inducing activity. Here, we report on the identification and characterization of BcXYG1, a secreted Glycoside Hydrolase Family 12 (GH12) xyloglucanase and an apoplastic protein with strong necrosis-inducing activity. We show that the BcXYG1 death-inducing signal is mediated by the plant LRR receptor-like kinases BAK1 and SOBIR1, that in addition to the induction of cell death, BcXYG1 is recognized by the plant immune system and activates defense responses, and that the enzymatic activity is not necessary for the induction of either cell death or plant defense responses.

RESULTS

The *B. cinerea* Secretome Contains Necrosis-Inducing Proteins

Fungal effectors and virulence proteins are expressed specifically during the infection stages in which they play a role. Therefore, we developed a system to collect the fungal secretome from inoculated plants, expecting it to be enriched for in planta-expressed plant-affecting proteins. According to our *B. cinerea* infection model, we expect that it uses necrosis-inducing molecules at the early infection stage (Shlezinger et al., 2011). Therefore, we anticipated necrosis-inducing activity in

[1] This work was supported by BARD grant numbers CA9122-09 and IS4937-16 to A.Sh.

[2] Address correspondence to amirsh@ex.tau.ac.il.

The author responsible for distribution of materials integral to the findings presented in this article in accordance with the policy described in the Instructions for Authors (www.plantphysiol.org) is: Amir Sharon (amirsh@ex.tau.ac.il).

W.Z. was supported in part by the National Natural Science Foundation of China (31501587). G.M. was supported in part by a fellowship from the Edmond J. Safra Center for Bioinformatics at Tel-Aviv University. N.B.-T. acknowledges the support of grant no. 1775/12 of the I-CORE Program of the Planning and Budgeting Committee and The Israel Science Foundation. Funding of O.V. and G.H.B. was provided by the Deutsche Forschungsgemeinschaft (DFG).

W.Z. designed and performed most of the experiments, analyzed the data and wrote the manuscript; M.R. performed all the early screening and proteomic analyses; Y.R. initiated the project and established the scientific system; A.M.-D. performed the work associated with CA-Rac strain; G.M. and N.B-T. assisted in protein structure analyses; A.S, O.V., and G.H.B. performed the proteomic analyses; K.B. and M.B.-P. performed enzymatic activity assays; A.S. conceived the project and wrote the article with contributions of all the authors.

www.plantphysiol.org/cgi/doi/10.1104/pp.17.00375

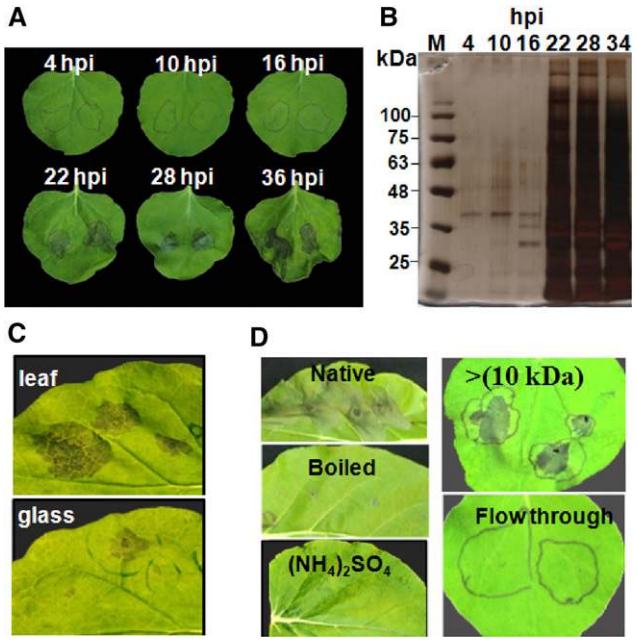

Figure 1. Necrosis-inducing activity of the *B. cinerea* secretome. A, Bean leaves were inoculated with a suspension of *B. cinerea* spores. At the designated time points post inoculation, the suspension was collected and centrifuged, the spores and mycelia fragments were removed by filtering through 45-μm filters, and the clean suspension was infiltrated into *N. benthamiana* leaves. Images show leaves 3 d after treatment. B, Clean spore suspension was boiled and mixed with loading buffer, 20 μL was loaded onto an SDS-PAGE gel and separated by electrophoresis, and the gel was stained with silver reagent. C, Suspension was collected from inoculated bean leaves or from a fungus that was grown in Gamborg's B5 on a glass slide. Images were taken 3 d after infiltration of leaves with the clean suspension. D, Clean suspension was treated by boiling for 10 min, precipitation of proteins with ammonium sulfate, or dialysis through a 10-kD membrane. Images were taken 3 d after infiltration of leaves with boiled suspension (Boiled), suspension after protein precipitation [$(NH_4)_2SO_4$], dialyzed suspension (10 kDa), or the flow through after dialysis (Flow through).

the fungal secretome collected from leaves rather early after inoculation, and indeed, the purified *B. cinerea* secretome caused necrosis in *N. benthamiana* leaves as early as 22 hpi (Fig. 1A), coinciding with a steep increase in the amount of secreted proteins (Fig. 1B). Based on the activity and protein amounts, we selected the 28-hpi time point for all further analyses. When the fungus was grown on a glass slide for the same period of time, it developed comparable amounts of mycelia; however, the necrosis-inducing activity of the secretome from glass-grown fungus was much weaker (Fig. 1C), supporting the enrichment of the leaf-collected secretome with necrosis-inducing factors. In addition to *N. benthamiana*, the secretome caused necrosis in all other plant species that we examined, including maize (*Zea mays*) and wheat (data not shown). Induction of necrosis was lost when the secretome was boiled or when proteins were precipitated with ammonium sulfate and retained within the tubes following ultrafiltration through 10 kD (Fig. 1D), confirming that the necrosis is induced by secreted proteins.

Proteomic Analysis of the Secretome

A total of 259 secreted proteins were identified in the secretome of the wild-type strain (Supplemental Table S1). The largest groups included enzymes of carbohydrate hydrolysis, proteins of unknown function, cell wall-degrading enzymes, oxidoreductase, and proteases (Supplemental Fig. S1). Besides minor differences in percentages, the overall partitioning of the proteins among functional categories was similar to previously reported analyses of the *B. cinerea* secretome (González et al., 2016). To identify potential NIPs, we compared the wild-type secretomes and two pathogenicity mutants. The first was Δ*bcnoxA*, which has a deletion of the NADPH oxidase catalytic subunit. This strain is able to penetrate host tissue in the same way as the wild type but shows much slower spreading and plant colonization (Segmüller et al., 2008). The second was CA-BcRAC, a strain expressing a constitutively active (CA) allele of the small GTPase BcRAC, which causes earlier and more intense necrosis than the wild type (Minz-Dub et al., 2013). Comparing the presence and abundance of proteins among the different strains (Supplemental Tables S2 and S3) allowed us to exclude certain proteins and to categorize others as high or low priority. Additional criteria used to prioritize candidate proteins were peptide abundance, presence of a secretion signal, predicted function, and M_r of the protein (600 or fewer amino acids). The first 20 proteins in the priority list were screened by *Agrobacterium tumefaciens* infiltration assay of *N. benthamiana* leaves (Supplemental Table S4), and among them, we found BC1G_00594, which showed strong necrosis-inducing activity and was characterized further.

BC1G_00594 Is a GH12 Protein

The *B. cinerea BC1G_00594* is a single-copy gene consisting of four exons and three introns. The first 18 N-terminal amino acids encode a signal peptide, and the entire predicted protein includes 248 amino acids with two Cys residues (C^{33} and C^{61}). No transmembrane helices of this protein were predicted using TMHMM Server version 2.0 (http://www.cbs.dtu.dk/services/TMHMM/), indicating that the protein encoded by *BC1G_00594* is secreted, as is also evident from its presence in the *B. cinerea* secretome. BLAST searches of fungal genomes with BC1G_00594 showed the presence of homologs in a large number of necrotrophic and hemibiotrophic plant pathogens as well as in saprotrophic fungal species, but we could not find homologs of the protein in biotrophic plant pathogens, including *Blumeria graminis* f. sp. *hordei*, *Ustilago maydis*, and *Puccinia* spp., or in the human pathogen *Candida albicans*. Multiple sequence alignment and phylogenetic analysis revealed significant sequence conservation (Supplemental Fig. S2, A and B), especially

of the two Cys residues, which are well conserved in all of the BC1G_00594 homologs (Supplemental Fig. S2A). These Cys residues are possibly involved in the formation of disulfide bonds (Sevier and Kaiser, 2002) and, therefore, might play a significant role in the structure and function of the protein. Prediction of the 3D structure of the BC1G_00594 protein using I-TASSER showed that it shares strong structural similarity with XEG1, a GH12 protein (XP_009525815.1) from *P. sojae* that is important for virulence (Ma et al., 2015). BLAST search of the *B. cinerea* genome in the JGI database uncovered another GH12 protein (BC1G_01008) with relatively low similarity to BC1G_00594 and other necrosis-inducing GH12 proteins (Supplemental Fig. S3). We named the BC1G_00594 protein BcXYG1, as, to our knowledge, this is the first report of a *B. cinerea* xyloglucanase, and the BC1G_01008 protein BcXYG2.

BcXYG1 Induces Cell Death in Dicot Plants

We examined the necrosis-inducing activity of BcXYG1 in plants other than *N. benthamiana*. To avoid possible effects on protein production by *A. tumefaciens* compatibility, BcXYG1 was produced in *Escherichia coli* (Fig. 2A), and the purified protein was infiltrated to leaf mesophyll using a syringe. Treatment of *N. benthamiana* leaves with BcXYG1 concentrations ranging from 10 to 200 μg mL^{-1} resulted in strong necrosis at all of the tested concentrations (Fig. 2B), unlike either EGFP or BcXYG2, which had no effect even at 100 μg mL^{-1} (Fig. 2C). Similar results were obtained with additional dicot plants, including tomato and bean (*Phaseolus vulgaris*), but not in monocot plants, including maize and wheat (Fig. 2D). Hence, BcXYG1 has a strong necrosis-inducing activity in dicot plants, but similar to other *B. cinerea* NIPs, it does not promote necrosis in cereals (Fig. 2D).

Induction of Necrosis Is Independent of the Glycosyl Hydrolase Activity of BcXYG1

In *Trichoderma reesei* GH12 protein, two highly conserved catalytic residues, E^{116} and E^{200}, are essential for the xyloglucan-hydrolyzing activity (Sandgren et al., 2005). The corresponding catalytic residues in *B. cinerea* BcXYG1 are E^{142} and E^{229} (Supplemental Fig. S2A). In addition, certain CWDEs can trigger plant cell death, and in a few cases, the enzymatic activity was found to be unrelated to the cell death-inducing activity

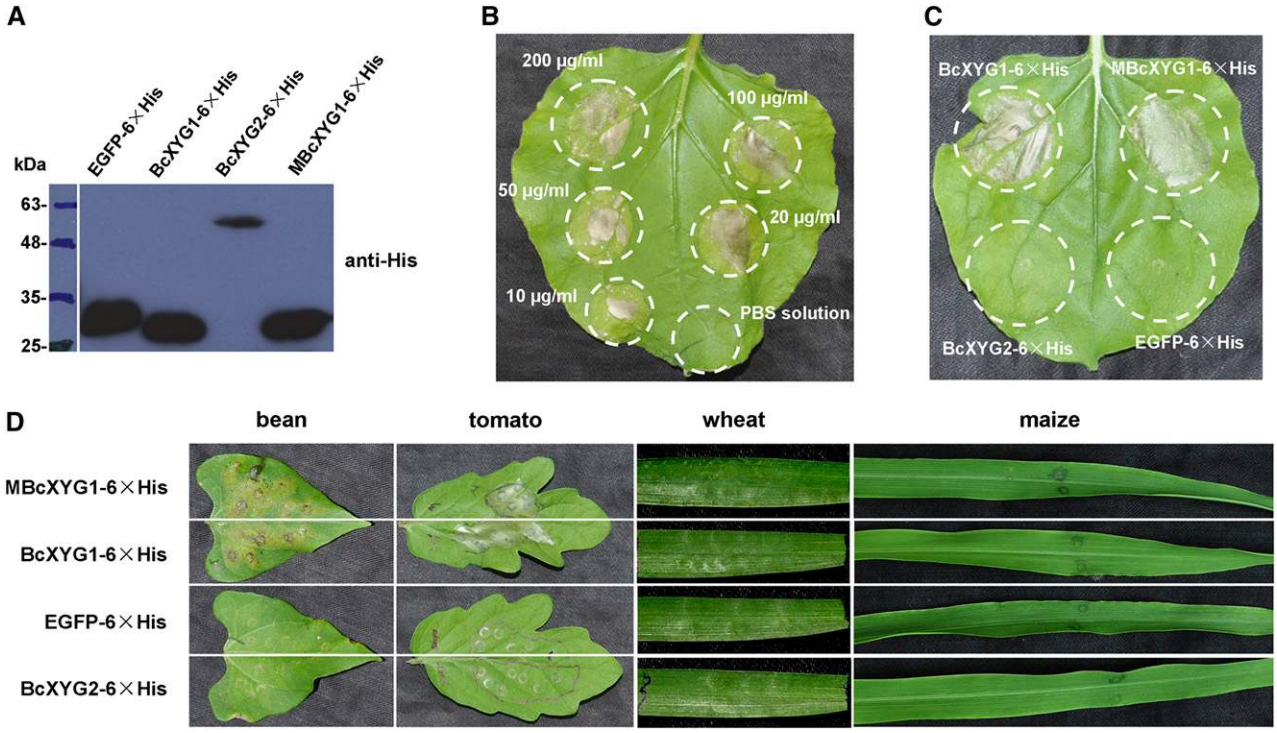

Figure 2. Purified BcXYG1 induces necrosis in multiple plants. *BcXYG1* and control proteins fused to 6× His were expressed in *E. coli*, purified, suspended in phosphate-buffered saline (PBS), and infiltrated into leaves. A, Immunoblot analysis of proteins expressed in *E. coli* using anti-His antibodies. EGFP-6×His, EGFP (negative control); BcXYG1-6×His, native BcXYG1; MBcXYG1-6×His, mutant BcXYG1 that lacks enzymatic activity; BcXYG2-6×His, BcXYG1 homolog that lacks necrosis-inducing activity. B, Response of *N. benthamiana* leaves to different concentrations of BcXYG1-6×His. C, Treatment of *N. benthamiana* leaves with 100 μg mL^{-1} purified proteins. D, Treatment of bean, tomato, wheat, and maize leaves with 100 μg mL^{-1} purified proteins. Images in B to D were taken 5 d after treatment.

(Furman-Matarasso et al., 1999; Poinssot et al., 2003; Noda et al., 2010; Zhang et al., 2014b; Ma et al., 2015). To determine if the hydrolase activity of BcXYG1 is necessary for the induction of necrosis, we mutated E^{142} and E^{229} to Gln using site-directed mutagenesis. Enzymatic assays with purified mutated protein (MBcXYG1) showed complete loss of the xyloglucan-degrading endoglucanase activity (Supplemental Fig. S4A). Infiltration of *N. benthamiana* with purified mutant protein (Fig. 2C) or *A. tumefaciens* infiltration assay (Supplemental Fig. S4B) both showed that the MBcXYG1 mutant protein retained full necrosis-inducing activity. Infiltration of leaves with purified MBcXYG1 protein also induced cell death in additional dicot plants, but not in wheat and maize, similar to the effects of wild-type BcXYG1 (Fig. 2D). These results confirm the xyloglucanase activity of BcXYG1 and show that it is not necessary for the induction of plant cell death by BcXYG1.

BcXYG1 Is Active Outside of the Plant Cell

To verify the secretion of BcXYG1, we generated *B. cinerea* strains overexpressing *BcXYG1-HA*, cultured them in potato dextrose broth (PDB) liquid medium, and checked for the presence of the protein in the culture filtrate. Western-blot analysis confirmed the accumulation of the BcXYG1-HA fusion protein in the culture medium (Fig. 3A), providing conclusive proof that BcXYG1 is secreted by the fungus. To determine if BcXYG1 triggers cell death by interaction with extracellular or intracellular targets, we constructed *A. tumefaciens* strains expressing BcXYG1 with and without a secretion signal. Two constructs were produced: (1) the N-terminal signal peptide of BcXYG1 was replaced with the Arabidopsis PR3 signal peptide (TAIR identifier AT3G12500) to produce PR3 SP-BcXYG1$^{19\text{-}248}$-HA; and (2) the signal peptide was deleted to produce ATG-BcXYG1$^{19\text{-}248}$-HA. The PR3 SP-Nep1$^{21\text{-}246}$-HA fusion was used as a positive control, and the PR3 SP-BcXYG2$^{23\text{-}398}$-HA (a homolog of BcXYG1 that does not induce necrosis) fusion protein was used as a negative control (Fig. 3, B and D). Immunoblot analysis confirmed that all the examined proteins were expressed in *N. benthamiana* following *A. tumefaciens*-mediated transient expression (Fig. 3C). Plants treated with *A. tumefaciens* expressing either PR3 SP-BcXYG1$^{19\text{-}248}$-HA or PR3 SP-Nep1$^{21\text{-}246}$-HA fusion protein, both of which are secreted from the plant cells to the apoplast, developed the typical necrosis, whereas the expression of ATG-BcXYG1$^{19\text{-}248}$-HA, which lacks the signal peptide and, therefore, remains inside the cell, did not trigger cell death (Fig. 3D). These results indicate that BcXYG1 triggers cell death by interacting with extracellular components, either in the cell wall or the cell membrane.

BcXYG1 Does Not Affect Fungal Growth, Colony Morphology, and Stress Tolerance

To determine the possible effects of *BcXYG1* on fungal development and pathogenicity, we generated *BcXYG1* deletion strains (Δ*xyg1-1* and Δ*xyg1-2*) and strains that overexpress either the native protein (OEXYG1) or the enzymatic activity mutant protein (OEMXYG1) and characterized their phenotypes. Deletion and overexpression of the gene and protein were confirmed by PCR, quantitative reverse transcription (qRT)-PCR, and western-blot analyses, respectively (Fig. 3A; Supplemental Fig. S5). No differences in colony morphology and growth rate on potato dextrose agar (PDA) were identified in any of the mutant strains as compared with wild-type cultures (Supplemental Fig. S6, A and B). In addition, there was no difference between the mutants and the wild-type control in sensitivity to different types of stresses, including salt stress (1 M NaCl), osmotic stress (1 M sorbitol), and cell wall stress (0.3 mg mL^{-1} Calcofluor White, 0.02% SDS, and 0.5 mg mL^{-1} Congo Red; data not shown). Native, but not heat-denatured, secretome of the wild type and Δ*xyg1* strains had similar necrosis-inducing activity in tobacco and maize leaves (Supplemental Fig. S6C), indicating that other NIPs can compensate for the loss of BcXYG1.

BcXYG1 Is Highly Expressed at the Early Infection Stage

Transcript levels of *BcXYG1* increased rapidly following the inoculation of leaves and reached a peak of about 40-fold compared with 0 at 12 hpi. The transcript levels then dropped sharply, to a level that was slightly higher than the initial level (Fig. 4). When *B. cinerea* was grown on solid Gamborg's B5 medium, the expression levels of *BcXYG1* remained stable until 12 hpi and then increased gradually, reaching a maximum of about 12-fold increase compared with 0 at 48 hpi (Fig. 4). The expression pattern of *BcXYG2* also increased rapidly following the inoculation of leaves and peaked around 36 hpi, but it increased only about 9-fold, compared with a 40-fold increase of *BcXYG1*. On solid medium, the expression level of *BcXYG2* started to increase around 12 hpi, reaching a similar level to its expression levels on plants around 60 hpi. The early and high induction of *BcXYG1*, but not *BcXYG2*, on plants supports a role of BcXYG1 in the pathogenicity of *B. cinerea*, possibly as a factor that is necessary for the establishment of primary lesions during the early infection stage.

BcXYG1 Contributes to the Production of Local Necrosis during Early Fungal Establishment

According to our working model, NIPs facilitate the production of local necrosis during the early stage of infection. The early expression of *bcxyg1* in planta further supports a role of the protein in the generation of local necrosis, which is used for the establishment of the infection court. To compare the pathogenicity of the wild-type and *bcxyg1* transgenic strains, beans leaves were inoculated with spores of the different strains and lesion size was measured 72 hpi. A slightly larger lesion was produced by the overexpression strains; however, the differences were statistically insignificant (Supplemental Fig. S7), suggesting that deletion or overexpression of *BcXYG1* does not affect

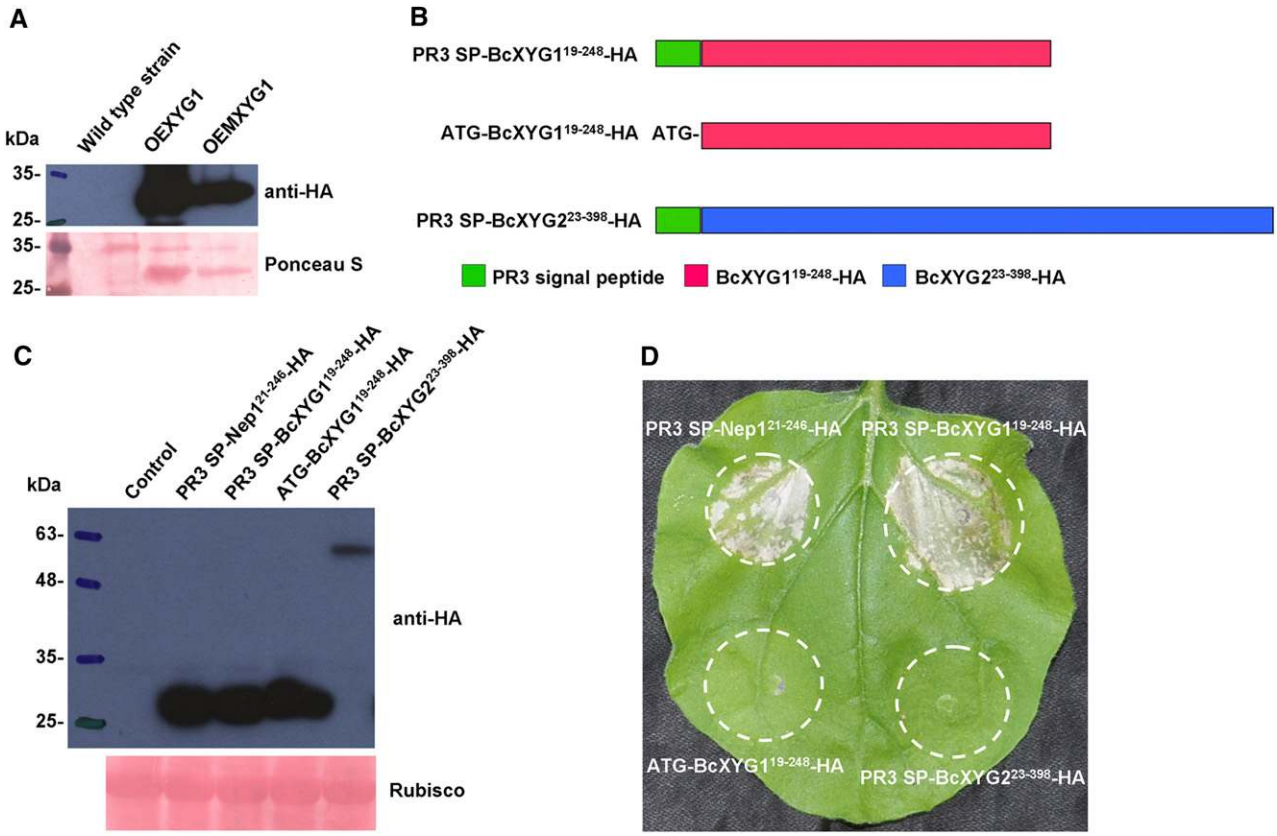

Figure 3. BcXYG1 is secreted to and is active in the plant apoplast. A, *B. cinerea* strains were cultured in liquid PDB medium for 48 h, the culture filtrate was collected and purified by filtration, and 20 μL was analyzed by gel electrophoresis and immunoblot using anti-HA antibodies. Top gel, Immunoblot using anti-HA antibodies; bottom gel, Ponceau S staining of total proteins. B to D, Analysis of necrosis produced by *A. tumefaciens* strains transiently expressing *BcXYG1* with and without secretion signal. B, Schematic presentation of the examined constructs. PR3 SP-BcXYG$^{19-248}$-HA, HA-tagged BcXYG1 with the native signal peptide replaced by Arabidopsis PR3 secretion signal; ATG-BcXYG$^{19-248}$-HA, HA-tagged BcXYG1 lacking the native secretion signal; PR3 SP-BcXYG$^{23-398}$-HA, HA-tagged BcXYG2 (does not induce necrosis) with the native secretion signal replaced by the Arabidopsis PR3 secretion signal. C, Immunoblot analysis of proteins from *N. benthamiana* leaves transiently expressing the various constructs. PR3 SP-Nep1$^{21-246}$-HA, HA-tagged BcNep1-HA with the native secretion signal replaced by Arabidopsis PR3 secretion signal; Control, *N. benthamiana* leaves infiltrated with GV3101 carrying a pCAMBIA3300 empty vector. Top gel, Immunoblot using anti-HA antibodies; bottom gel, Ponceau S staining of the Rubisco large subunit. D, Images of *N. benthamiana* leaves 5 d after infiltration with the various *A. tumefaciens* strains.

the final outcome of infection. To gain insight into possible unnoticed effects caused by BcXYG1, particularly during the early infection stage, we characterized infection of the *bcxyg1* overexpression and deletion strains using the PathTrack system. This system allows for sensitive and quantitative analysis of infection dynamics and, therefore, can reveal small changes in disease development (Eizner et al., 2017). The pathogenic behavior of the Δ*bcxyg1* deletion strain was similar to that of the wild type in all of the examined parameters, including time and magnitude of early necrosis, break time, and lesion expansion rate (Fig. 5). This result might not be surprising, considering that the secretome contains additional NIPs that can compensate for the lack of BcXYG1 (as shown in Supplemental Fig. S6C). The OEXYG1 and OEMXYG1 strains both produced significantly earlier and more intense local necrosis and had slightly earlier, but statistically insignificant, break times than the wild-type strain (Fig. 5). All of the examined strains, including the wild type, the deletion, and the different overexpression strains, had similar lesion expansion rates, which can explain the similar final lesion size at 72 hpi.

BcXYG1 Triggers PTI and Induces Systemic Resistance in Bean

Recent reports showed that at least some necrosis-inducing proteins are recognized by the plant immune system and can activate PTI (Zhang et al., 2014b; Frías et al., 2016). To assess whether BcXYG1 could induce resistance in addition to cell death, one of two primary bean leaves was infiltrated with 100 μg mL^{-1} BcXYG1 or MBcXYG1, and after 2 d, the second, untreated leaf was inoculated with *B. cinerea*. In plants that were

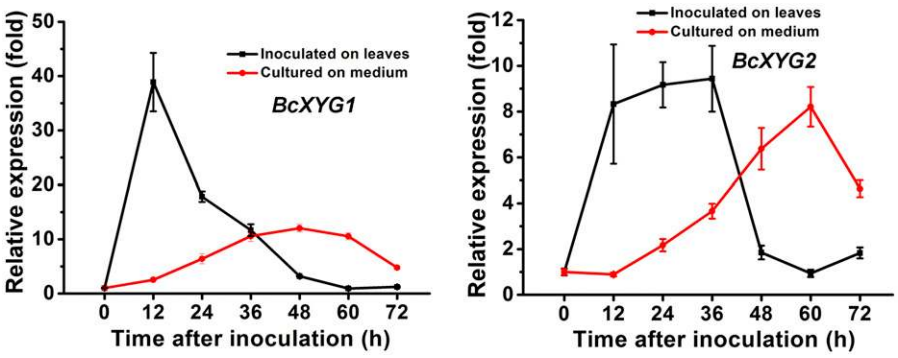

Figure 4. *BcXYG1* is highly expressed following plant inoculation. Bean leaves (black lines) or Gamborg's B5 medium (red lines) were inoculated with *B. cinerea* spores, and expression levels of the *BcXYG1* and *BcXYG2* genes were evaluated by qRT-PCR. The expression level of *BcXYG1* and *BcXYG2* inoculated on plants or in Gamborg's B5 medium at 0 h was set as 1, and relative levels of transcript were calculated using the comparative Ct method. Transcript levels of the *B. cinerea Bcgpdh* gene were used to normalize different samples. Data represent means and SD of three independent replications.

preinfiltrated with BcXYG1 or MBcXYG1, lesion size on the infected leaf was significantly smaller compared with lesions size on leaves in untreated plants or plants that were preinfiltrated with BcXYG2 or EGFP (Fig. 6A). Reverse transcription-PCR analysis of gene expression in untreated leaves showed marked increases of the plant defense genes *Pvd1* (GenBank accession no. HM240258.1), *PvPR1* (GenBank accession no. CAA43637.1), and *PvPR2* (GenBank accession no. CAA43636.1) following infiltration of the other leaf with BcXYG1 or MBcXYG1, compared with a modest increase in plants that were pretreated with BcXYG2, EGFP, or blank (Fig. 6B). These results show that BcXYG1 induces systemic resistance in bean plants, which is independent of its xyloglucanase activity. Interestingly, although BcXYG1 and MBcXYG1 both induced similar levels of necrosis and triggered systemic resistance, the expression levels of defense genes in BcXYG1-pretreated plants were significantly higher than in MBcXYG1-pretreated plants (Fig. 6B). This result suggests that the xyloglucan hydrolysis products produced by BcXYG1 also contribute to the induction of plant defense.

The Necrosis-Inducing Activity of MBcXYG1 Is Dependent on Its Tertiary Structure

Previous studies demonstrated that certain plant cell wall residues, such as oligogalacturonides and oligosaccharides that are released by enzymatic hydrolysis, could activate plant defense responses (Ferrari et al., 2013; Trouvelot et al., 2014; Benedetti et al., 2015; Wu et al., 2016). To eliminate the possible effect of xyloglucan hydrolysis products on plant systemic resistance, we used the xyloglucanase activity mutant MBcXYG1 for subsequent studies.

Denaturation of BcXYG1 by incubation at 95°C for 15 min abolished the necrosis-inducing activity (Fig. 7A), indicating that the tertiary structure of BcXYG1 is important for this function. Structural analysis of BcXYG1 using PredictProtein (https://www.predictprotein.org/) predicted the formation of an intramolecular disulfide bond by Cys residues C^{33} and C^{61} (Supplemental Fig. S2A), which are essential for protein folding and for maintenance of the tertiary structure (Sevier and Kaiser, 2002; Marianayagam et al., 2004). To verify if the necrosis-inducing activity of BcXYG1 depends on its intact tertiary structure, we replaced MBcXYG1 C^{33} and C^{61} with Ala, either individually or simultaneously. In addition, we deleted the last 12 amino acids (VFKTTAYSVSLN; amino acids 237–248) of the protein, which constitute a β-strand that is important for maintaining the structural integrity and stability of BcXYG1 (Fig. 7D). All of the examined mutations resulted in complete loss of the necrosis-inducing activity of the protein, as demonstrated by the *A. tumefaciens* infiltration assay of *N. benthamiana* (Fig. 7, B–F). Hence, disruption of the tertiary structure destroys the necrosis-inducing activity of BcXYG1.

Previous studies reported that two surface-exposed loops comprise a conserved two-peptide motif on the surface of the elicitor BcSpl1. The two motifs interact with each other to form a small protrusion on the protein surface and contribute synergistically to the triggering of necrosis (Frías et al., 2014), indicating that proper space distance and position of the active epitope motifs are important for the necrosis-inducing activity of this protein (Frías et al., 2014). Analysis of the surface accessibility of BcXYG1 using ASA-View (http://www.abren.net/asaview/) showed that the peptides GSN (amino acids 118–120) and SETGS (amino acids 157–161) are surface exposed (Supplemental Fig. S8) and constitute two protrusive loop structures on the surface of the protein (Supplemental Fig. S3C). In addition, these two short stretches are not conserved in BcXYG2 (Supplemental Fig. S3A), implying that either or both of the peptides $GSN^{118\text{-}120}$ and $SETGS^{157\text{-}161}$ might be important for the necrosis-inducing activity of BcXYG1. To verify this possibility, we replaced the residues $GSN^{118\text{-}120}$ with $AAA^{118\text{-}120}$ and the residues $SETGS^{157\text{-}161}$ with $AAAAA^{157\text{-}161}$, individually or simultaneously, and transiently expressed the mutant proteins in *N. benthamiana*

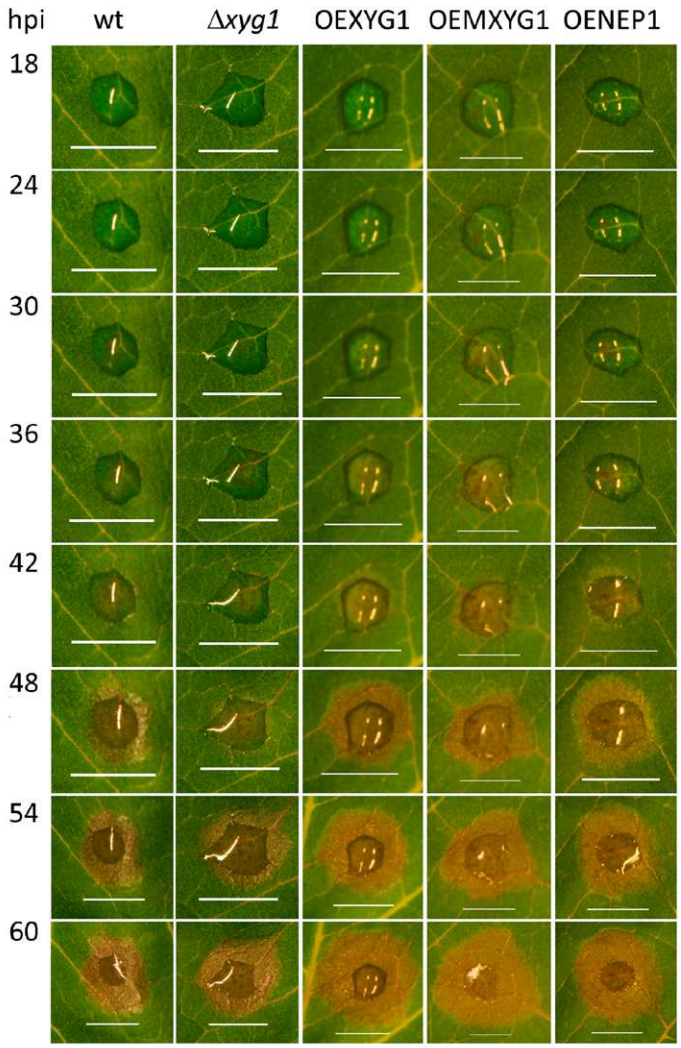

	wt	Δ*xyg1*	OEXYG1	OEMXYG1	OENEP1
1st necrosis (hpi)	26.50 ±1.91	26.70 ±1.50	17.25 ±2.22	18.50 ±2.52	20.50 ±2.89
Break (hpi)	43.62 ±2.62	44.12 ±2.46	39.25 ±0.96	40.50 ±3.41	39.50 ±1.73
Expn. Rate (mm/h)	0.159 ±0.018	0.167 ±0.008	0.158 ±0.027	0.167 ±0.008	0.177 ±0.020

Figure 5. BcXYG1 contributes to the establishment of the infection in early stages of pathogenic development. Bean leaves were inoculated with spores of the different strains, the leaves were photographed every 10 min, and the data were analyzed using PathTrack (Eizner et al., 2017). Images show selected time points during pathogenic development. Note the earlier and more intense appearance of local lesions in overexpression strains. The data show averages of time of first necrosis (1st necrosis), time when lesion spreading starts (Break), and lesion expansion rate (Expn. Rate). Data represent means and SD from four independent experiments each with the wild type and one of the mutants. The appearance of the first necrosis was significantly earlier ($P \leq 0.05$) in all the overexpression strains than in the wild type and was similar between the deletion and wild-type strains, according to one-way ANOVA. The break time of the overexpression strains was slightly earlier than the break time of the wild-type strain; however, the differences were statistically insignificant ($P \leq 0.05$). Strain designations are as follows: wt, B05.10 wild-type strain; Δ*bcxyg1*, deletion of the *bcxyg1* gene; OEXYG1, overexpression of the native *bcxyg1* gene; OEMXYG1, overexpression of the mutated (no enzymatic activity) *bcxyg1* gene; OENEP1, overexpression of the *bcnpp1* gene (NEP1). Bars = 5 mm.

leaves using *A. tumefaciens* infiltration. Neither the $GSN^{118\text{-}120}$ nor the $SETGS^{157\text{-}161}$ mutation alone had an effect on the necrosis-inducing activity of the protein, but simultaneous mutation of both sites completely abolished it (Fig. 8, A and B). Furthermore, simultaneous mutation of two other pairs of surface-exposed peptides, $TGSY^{41\text{-}44}/TSNS^{68\text{-}71}$ and $WNITG^{51\text{-}55}/GGSSQ^{82\text{-}86}$, did not affect necrosis-inducing activity (Fig. 8, A and B). Hence, both the $GSN^{118\text{-}120}$ and $SETGS^{157\text{-}161}$ motifs are necessary for the induction of necrosis by BcXYG1, and each of them alone is sufficient for full necrosis-inducing activity. Integration of the $GSN^{118\text{-}120}$ and $SETGS^{157\text{-}161}$ motifs into BcXYG2 did not confer necrosis-inducing activity in this protein (Fig. 8, C–E), suggesting that additional properties, such as proper space distance and position of the active epitope motifs, are critical for the necrosis-inducing activity, as was found in the NIP BcSpl1 (Frías et al., 2014).

Defense Stimulation by BcXYG1 Is Unrelated to Necrosis-Inducing Activity

We used the $GSN^{118\text{-}120}/SETGS^{157\text{-}161}$ mutant protein to test if necrosis is necessary for induced plant defense. Bean leaves were infiltrated with the $MBcXYG1^{(GSN118\text{-}120AAA\ SETGS157\text{-}161AAAAA)}$ protein, and the other leaf was inoculated with *B. cinerea* as described above. The $MBcXYG1^{(GSN118\text{-}120AAA\ SETGS157\text{-}161AAAAA)}$ protein induced systemic resistance similar to that induced by MBcXYG1, as determined by lesion size and the expression of defense genes (Fig. 9). Hence, the abolishment of necrosis-inducing activity did not abolish the activation of the plant defense system by BcXYG1, suggesting that the plant immune response is triggered by the recognition of BcXYG1 and not by the necrosis that is cause. To verify this possibility, we tested the effect of Dukatalon (132 g L^{-1} paraquat and 66 g L^{-1} diquat), an

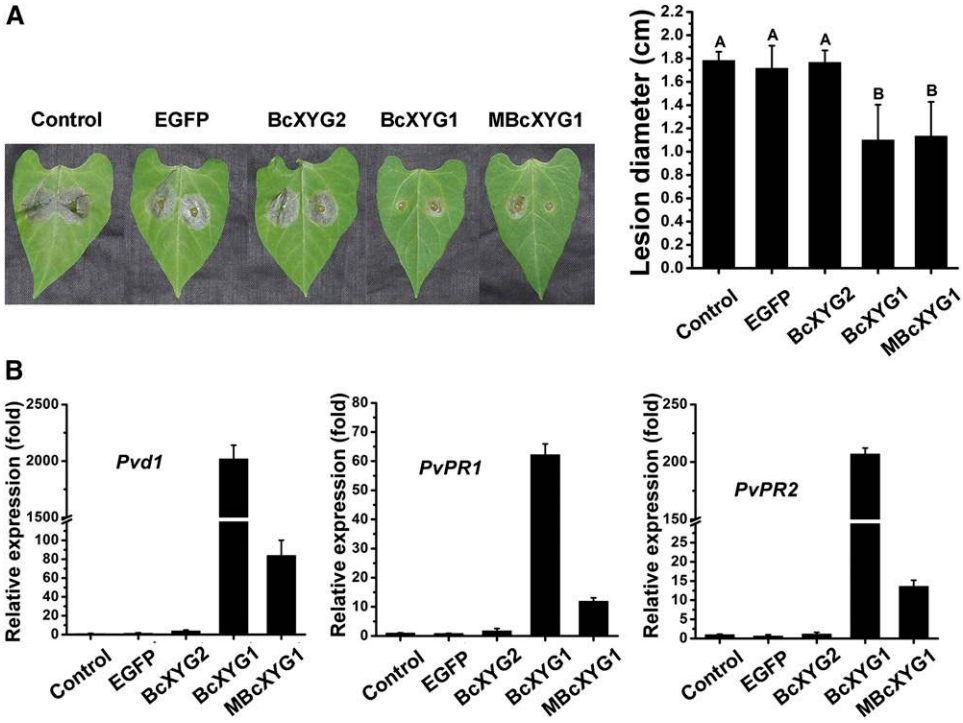

Figure 6. BcXYG1 induces resistance in bean. A, One of the first two true leaves of a 9-d-old bean seedling was infiltrated with 500 μL of purified protein solution. The plants were kept in a growth chamber for 48 h, the second leaf was then inoculated with wild-type *B. cinerea* spores, and the plants were kept in a humid environment. Photographs were taken (left) and average lesion size was determined (right) 72 hpi. Data represent means and SD from three independent experiments, each with six replications. Different letters in the graph indicate statistical differences at $P \leq 0.01$ using one-way ANOVA. B, Untreated leaves were picked 48 h after treatment, and relative expression levels of the defense genes *Pvd1*, *PvPR1*, and *PvPR2* were determined by qRT-PCR analysis. The expression level in blank control plants was set as 1. The expression level of the bean *Actin-11* gene was used to normalize different samples. Data represent means and SD of three independent replicates.

herbicide that induces necrosis, on the activation of plant resistance. Treatment with Dukatalon caused strong cell death in bean leaves, but it did not affect lesion size on the second leaf (Supplemental Fig. S9), indicating that the induction of necrosis is not the cause of defense activation. Additional experiments showed that the activation of plant defense is lost if the protein is denatured (by boiling) or destabilized (by peptide deletion; Supplemental Fig. S10). Therefore, we concluded that, similar to necrosis induction, the intact tertiary structure of BcXYG1 is necessary for the activation of plant defense, but the cell death- and defense-stimulating activities are probably mediated by different epitopes.

BcXYG1 Is Targeted to the Plant Membrane and Its Activity Is Mediated by BAK1 and SOBIR1

As demonstrated above, BcXYG1 needs to be in the plant extracellular space to induce cell death (Fig. 3D). To determine the site of action of BcXYG1 as either the plant cell wall or the cell membrane, tobacco protoplasts were incubated with 100 μg mL^{-1} MBcXYG1 (induces full necrosis) or MBcXYG1$^{(GSN118\text{-}120AAA\ SETGS157\text{-}161AAAAA)}$ (does not induce necrosis), and the number of intact protoplasts was counted. When incubated with MBcXYG1, the number of intact protoplasts decreased rapidly compared with protoplasts that were incubated with either MBcXYG1$^{(GSN118\text{-}120AAA\ SETGS157\text{-}161AAAAA)}$ or PBS (Fig. 10A). Within 1 h of incubation with MBcXYG1, protoplasts showed chloroplast disorganization and cell shrinkage and eventually disintegrated (Fig. 10B). This result shows that BcXYG1 does not need the cell wall to affect cells; hence, it probably targets the plasma membrane.

Many fungal effectors interact with plant receptor-like proteins (RLPs), which transmit the signals via the LRR receptor-like kinases SOBIR1 and BAK1 (Liebrand et al., 2013; Zhang et al., 2013, 2014b; Albert et al., 2015; Postma et al., 2016). Because BcXYG1 probably induces cell death through interaction with the plant cell membrane, it is possible that it is recognized by a membrane RLP and that the signal is mediated by an RLP-SOBIR-BAK1 complex. To address this possibility, we used virus-induced gene silencing (VIGS) to induce the gene silencing of *NbBAK1* or *NbSOBIR1* in *N. benthamiana* leaves. When infiltrated with MBcXYG1, the *NbBAK1*- or *NbSOBIR1*-silenced plants developed delayed symptoms, and the majority of the spots were either unaffected or developed late chlorosis (Fig. 11). Mature necrotic spots were observed in only

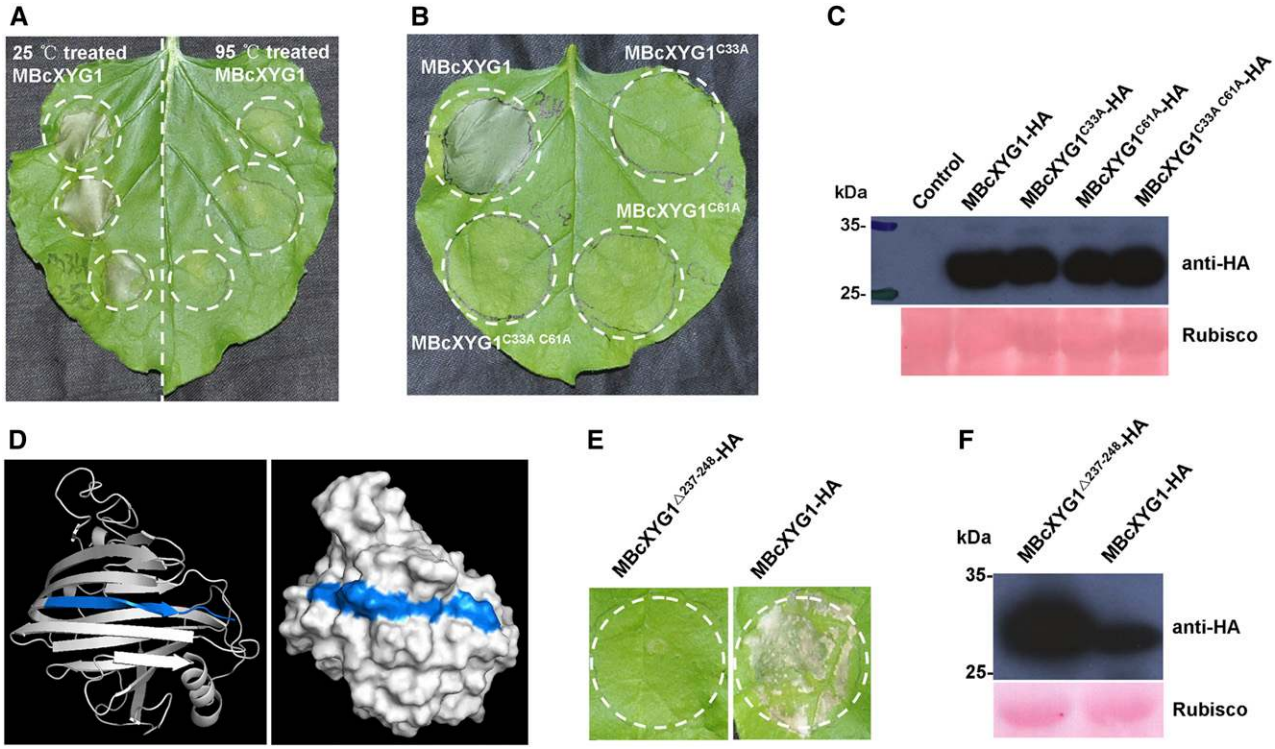

Figure 7. The necrosis-inducing activity of BcXYG1 is dependent on the protein tertiary structure. A, Assessment of the activity of denatured BcXYG1. Purified MBcXYG1 protein was incubated for 15 min at 25°C or 95°C. *N. benthamiana* leaves were treated with 100 μg mL^{-1} native (left) or denatured (right) proteins. Photographs were taken 5 d after the treatment of leaves. B, Assessment of the effect of destabilization of the tertiary structure on the activity BcXYG1. *N. benthamiana* leaves were infiltrated with *A. tumefaciens* strains expressing constructs of MBcXYG1 with mutations that destroy the tertiary structure of the protein. Photographs were taken 5 d after treatment. MBcXYG1^{C33A}-HA, Mutation in Cys residue 33; MBcXYG1^{C61A}-HA, mutation in Cys residue 61; MBcXYG1$^{C33A\ C61A}$-HA, mutation in both Cys residues 33 and 61. C, Immunoblot analysis of proteins from *N. benthamiana* leaves transiently expressing Cys residue mutants BcXYG1^{C33A}-HA, BcXYG1^{C61A}-HA, and BcXYG1$^{C33A\ C61A}$-HA from a pCAMBIA3300 vector. HA-tagged proteins were detected using anti-HA antibodies, Ponceau S-stained blots show the Rubisco large subunit. D, 3D structural models of BcXYG1 predicted using I-TASSER (http://zhanglab.ccmb.med.umich.edu/I-TASSER/) and analyzed further by PyMOL software. Left, Cartoon model of BcXYG1; right, surface model of BcXYG1. The 12 C-terminal amino acids constituting a β-strand structure (VFKTTAYSVSLN; amino acids 237–248) are depicted in blue. E, Effects of the destabilization of BcxYG1 by deletion of the 12 C-terminal amino acids. Photographs were taken 5 d after infiltration with an *A. tumefaciens* strain expressing either the mutant protein MBcXYG1$^{19\text{-}236(\Delta 237\text{-}248)}$-HA (left) or a native form of MBcXYG1 (right). F, Immunoblot analysis of proteins from *N. benthamiana* leaves transiently expressing either the 12 C-terminal amino acid deletion mutant MBcXYG1$^{19\text{-}236(\Delta 237\text{-}248)}$-HA or MBcXYG1.

28.57% and 46.15% of the *NbBAK1*- and *NbSOBIR1*-silenced leaves, respectively, compared with 100% necrotic spots in control plants or plants that were infiltrated with pTRV2-*GFP*. Interestingly, the *NbBAK1*-silenced leaves always showed a lower level of necrosis than the *NbSOBIR1*-silenced leaves. These results show that SOBIR1 and BAK1 mediate the necrosis-inducing activity of BcXYG1, possibly through an upstream RLP.

DISCUSSION

Upon first contact with a plant, necrotrophic pathogens face a dilemma: they have a limited capacity to extract nutrients from living tissues, yet they need to survive in a hostile live environment. Several reports have suggested that the solution might be a brief biotrophic phase that precedes the killing of plant cells and allows fungi such as *B. cinerea* and *Sclerotinia sclerotiorum* to subvert the host defenses and establish an initial infection court (Williams et al., 2011; Kabbage et al., 2013, 2015; van Kan et al., 2014). In our system, upon inoculation of leaves with *B. cinerea*, the spores germinate within a few hours and produce healthy and fully viable hyphae on the surface of the leaf within the first 24 hpi. Local microlesions then appear, concomitant with attempts of the fungus to penetrate into the tissue, followed by massive fungal cell death as a result of exposure of the fungal cells to the plant defense (Shlezinger et al., 2011). Therefore, we predicted that the initial infection stage of *B. cinerea* is mediated by cell death-promoting factors that the fungus delivers to the plant apoplast, which by instant killing of plant cell produce patches of dead tissue in which fungus is protected from the host defense and can used as initial

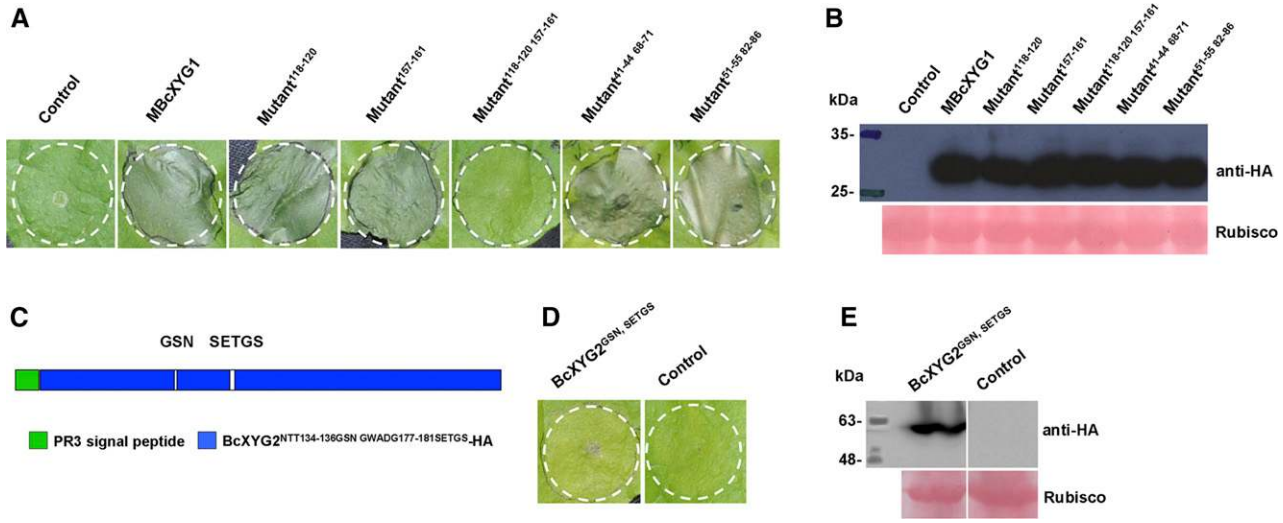

Figure 8. Induction of necrosis by BcXYG1 is mediated by two surface-exposed loop motifs. A, Effects of mutations in surface-exposed loops on the necrosis-inducing activity of BcXYG1. *N. benthamiana* leaves were infiltrated with *A. tumefaciens* strains expressing constructs with mutations in several different surface-exposed loops. Photographs were taken 5 d after treatment. B, Immunoblot analysis. HA-tagged proteins were detected using anti-HA antibodies. Ponceau S-stained blots show the Rubisco large subunit. C, Diagram of BcXYG2$^{NTT134-136GSN\ GWADG177-181SETGS}$-HA in which the BcXYG2 amino acids NTT$^{134-136}$ and GWADG$^{177-181}$ are substituted by the BcXYG1 amino acids GSN$^{118-120}$ and SETGS$^{157-161}$, respectively (BcXYG2$^{GSN\ SETGS}$). D, Activity assay of BcXYG2$^{GSN\ SETGS}$-HA. *N. benthamiana* leaves were infiltrated with *A. tumefaciens* carrying the BcXYG2$^{GSN\ SETGS}$-HA construct (left) or an empty vector (right). Photographs were taken 5 d after treatment. E, Immunoblot analysis. BcXYG2$^{GSN\ SETGS}$-HA was detected using anti-HA antibodies. Ponceau S-stained blots show the Rubisco large subunit.

infection courts. Here, we described the identification and analysis of BcXYG1, a plant cell death-promoting apoplastic effector found in the *B. cinerea* secretome collected from inoculated leaves 28 hpi. Initial tests with purified BcXYG1 showed that the necrosis-inducing activity of the protein is at least as strong as that of BcNEP1. Similar to BcNEP1 and other NIPs, the induction of necrosis by BcXYG1 is restricted to dicot plants, while the entire secretome could induce necrosis in both dicot and monocot plants, suggesting the presence of different classes of NIPs in the fungal secretome.

BcXYG1 is a CWDE xyloglucanase with a GH12 domain (Pfam identifier PF01670). CWDEs are the largest class of *B. cinerea*-secreted proteins, and many of the CWDEs found in our study, including BcXYG1, also were reported in previous proteomic analyses (Espino et al., 2010; González et al., 2016). In our work, we collected the secretome directly from leaves at a rather early time point (28 hpi) when, as we verified, the secretome has strong necrosis-inducing activity. Secretome from a fungus cultured on a glass slide had a significantly reduced necrosis-inducing activity compared with secretome from inoculated leaves, supporting the enhanced production of NIPs in planta. To assist in the identification of potentially important proteins present in the entire secretome, we compared secretomes from the wild type and pathogenicity mutants affected at different stages of infection. This approach allowed us to identify BcXYG1 as a potential NIP based on the relatively high abundance in the wild-type secretome and a further greater than 4-fold increase in secretome from a CA-BcRAC strain, which causes early and more intense necrosis (Minz-Dub et al., 2013). As could be expected, we also found high levels of previously identified NIPs in the secretome (Supplemental Table S1), including NPP1 (BC1G_10306), BcSpl1 (BC1G_02163), Xyn11A (B0510_640), BcGs1 (BC1G_04151), BcIEB1 (BC1G_12374), BcPG1 (BC1G_11143), BcPG2 (BC1G_02003), and BcPG3 (BC1G_04246; Cuesta Arenas et al., 2010; Noda et al., 2010; Frías et al., 2011, 2016; Zhang et al., 2014b, 2015). Interestingly, in the secretome collected from the CA-BcRAC strain, we also found high abundance of the NIPs NPP1 and BcSpl1 (Supplemental Table S3), which can explain the enhanced necrosis produced by this strain.

Taking several approaches, we showed that BcXYG1 is localized to the plant apoplast and that it targets the plant cell membrane (Figs. 3D and 10). Apoplastic effectors that induce cell death were reported recently in several systems, such as *Ustilaginoidea virens* and *Zymoseptoria tritici* (Fang et al., 2016; Kettles et al., 2017). Although BcXYG1 is a xyloglucanase, we showed that induction of cell death by BcXYG1 does not require the xyloglucan-degrading activity, suggesting that the cell death-inducing activity is mediated by a specific protein domain or motif. Treatment of protoplasts with a protein that lacks enzymatic activity (MBcXYG1) resulted in fast deterioration and death of the protoplasts, suggesting that recognition of BcXYG1 occurs on the cell membrane and may be mediated by an RLP. Silencing of *BAK1* and *SOBIR1* blocked the development of necrosis (Fig. 11),

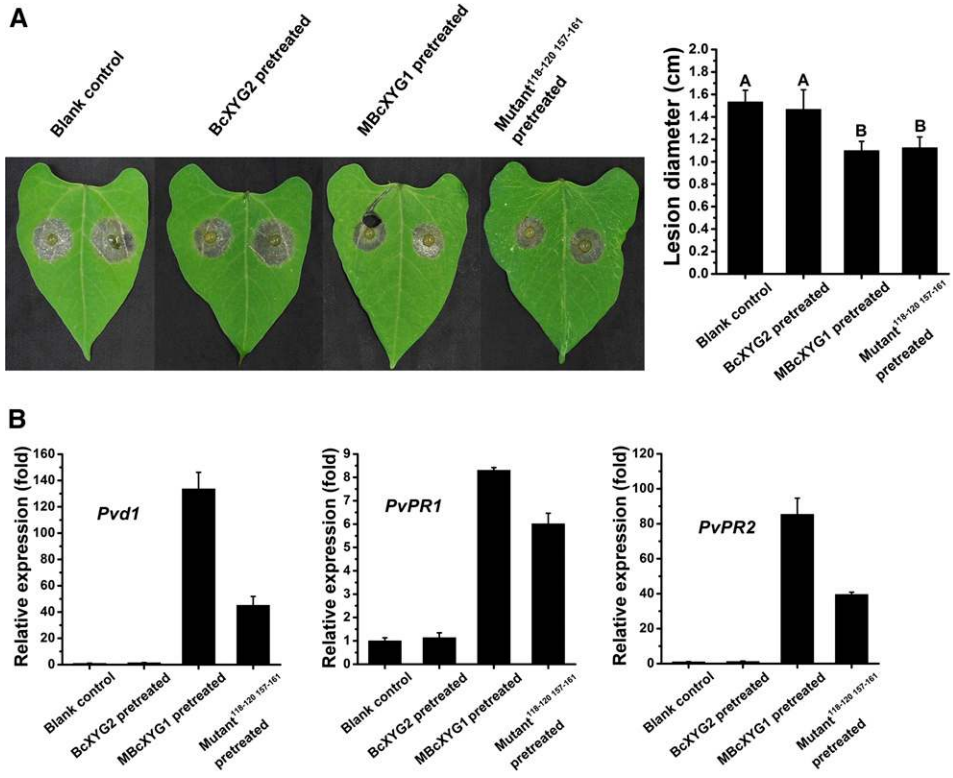

Figure 9. The necrosis-inducing activity of MBcXYG1 is not linked to plant defense-stimulating activity. A, One of the first two true leaves of 9-d-old bean seedlings was infiltrated with 500 μL of the indicated proteins at 100 μg mL^{-1}. After 2 d, the other leaf was inoculated with *B. cinerea*, the plants were incubated in a humid chamber, and the lesions were photographed and measured 72 hpi. Blank control, Untreated first leaf; BcXYG2, pretreatment with BcXYG2; MBcXYG1, enzyme-inactive BcXYG1 protein; Mutant$^{118\text{-}120\ 157\text{-}161}$, enzyme- and necrosis-inactive BcXYG1 protein in which the external loops 118 to 120 and 157 to 161 were mutated (MBcXYG1$^{GSN118\text{-}120AAA\ SETGS157\text{-}161AAAAA}$). Data represent means and SD from three independent experiments, each with six replications. Different letters in the graph indicate statistical differences at $P \leq 0.01$ using one-way ANOVA. B, Relative expression of defense genes. RNA was extracted from the untreated leaf 48 h after treatment of the first leaf, and the levels of the defense genes *Pvd1*, *PvPR1*, and *PvPR2* were determined by qRT-PCR. Expression in blank control plants was set as 1. The expression level of the bean *Actin-11* gene was used to normalize different samples. Data represent means and SD of three independent replicates.

supporting the possibility that an RLP-SOBIR1-BAK1 complex mediates the cell death-inducing activity of BcXYG1.

Studies of various NIPs showed that small epitopes located on the surface of the proteins are sufficient to induce necrosis, independent of the tertiary structure of the entire protein. For example, a 30-amino acid peptide on the surface of Xyn11A mediates the binding to plant cell membranes and the induction of cell death (Noda et al., 2010). Similarly, a 35-amino acid peptide derived from a conserved region of BcIEB1 is sufficient for triggering necrosis as well as for PTI (Frías et al., 2016). Heat-denatured *S. sclerotiorum* SsCut still could induce necrosis in tobacco leaves, and the entire C-terminal half of the protein was found to be indispensable for both enzymatic and elicitor activities (Zhang et al., 2014a). Denaturation of the polygalacturonase BcPG3 did not abolish the necrosis-inducing activity of this enzyme (Zhang et al., 2014b). In contrast to these examples, denaturation of BcXYG1 completely abolished both the induction of necrosis and defense-stimulating activities (Supplemental Fig. S10). Therefore, unlike many other studied NIPs, the tertiary structure of BcXYG1 is vital for the induction of both necrosis and PTI. In the case of necrosis-inducing activity, the intact tertiary structure of BcXYG1 is necessary to allow two loop domains (GSN [amino acids 118–120] and SETGS [amino acids 157–161]) to interact with each other on the surface of the protein. A similar situation was reported for the NIP BcSpl1, where two peptide motifs interact with each other to form a small protrusion on the protein surface, thereby synergistically contributing to the induction of necrosis (Frías et al., 2014). We have not identified a domain that mediates BcXYG1-activated PTI; therefore, it is unclear whether there is a specific domain or the entire protein is necessary for this activity.

Heat treatment or structural mutation of the *Pectobacterium carotovorum* pv *carotovorum*-derived NIP PccNLP abolished the induction of necrosis as well as the activation of plant defense by this effector (Ottmann et al., 2009; Böhm et al., 2014). In contrast, heat treatment or structural mutation of *Phytophthora*

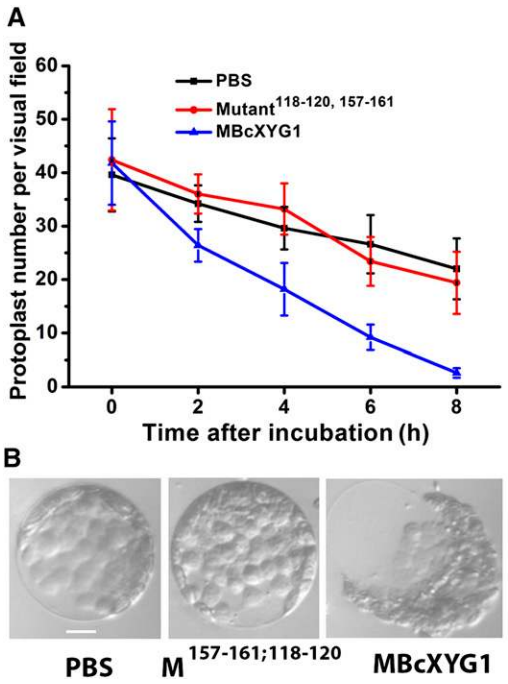

Figure 10. BcXYG1 triggers cell death on the plant cell membrane. *N. benthamiana* protoplasts were incubated with 100 μg mL^{-1} protein. A, The number of intact protoplasts was counted at the indicated time points. Data represent means and SD from three independent biological repeats with a total of 15 visual fields for each treatment. B, Images of tobacco protoplasts 1 h after the beginning of incubation. Bar = 10 μm.

parasitica PpNLP, a homolog of PccNLP, abolished the induction of necrosis but not of the plant defense (Böhm et al., 2014). *Hyaloperonospora arabidopsidis* HaNLP3, an NLP that lacks necrosis-inducing activity, acts as a potent activator of the plant immune system in Arabidopsis (Oome et al., 2014). Similarly, we found that the induction of cell death and plant defense by BcXYG1 are separable, as demonstrated by the MBcXYG1$^{(GSN118\text{-}120AAA\ SETGS157\text{-}161AAAAA)}$ mutant protein, which does not induce necrosis but retains PTI activity (Fig. 9). Collectively, our findings and work on additional cell death apoplastic NIPs show that induced cell death and plant defense activation are not always linked.

A number of apoplastic effectors interact with plant RLPs and deliver the signals via an RLP-SOBIR1-BAK1 complex (Liebrand et al., 2013; Zhang et al., 2013, 2014b; Albert et al., 2015; Du et al., 2015; Ma et al., 2015; Postma et al., 2016). Apoplastic effectors from the wheat pathogen *Z. tritici* were recently shown to induce NbBAK1- and NbSOBIR1-dependent cell death or chlorosis in nonhost *N. benthamiana* plants (Kettles et al., 2017), indicating the centrality of RLP-SOBIR1-BAK1 complexes in the recognition and delivery of the signals of apoplastic effectors. While BcXYG1 is not a classical effector (it does not target the immune system), we nevertheless showed that it is also targeted to the plant cell membrane, and its cell death effect is mediated by SOBIR1-BAK1. Hence, it is also logical to predict that BcXYG1 recognizes a yet unknown plant plasma membrane RLP, which mediates the signal. The *P. sojae* PsXEG1 (homolog of BcXYG1) affects the pathogenicity of this oomycete, and in this case, the enzymatic activity is required (Ma et al., 2015). A glucanase-inhibiting protein (GmGIP1) is produced by the plant and, specifically, blocks PsXEG1 as a means of defense (Ma et al., 2017b). PsXLP1, a class 2 GH12 and a homolog of PsXEG1 that lacks necrosis-inducing activity, also binds the plant GmGIP1, thereby counteracting the plant protection. It is thus possible to speculate that BcXYG2, which also is expressed at early infection stages but does not induce necrosis, might act as a BcXYG1 decoy that neutralizes putative BcXYG1-inhibiting plant proteins.

Multiple sequence alignment of BcXYG1 and additional GH12 proteins revealed higher similarity of BcXYG1 to necrosis-inducing GH12 proteins than to BcXYG2 (Supplemental Fig. S3A). Based on this analysis, we classified GH12 proteins into two groups, those that are more closely related to BcXYG1 and those that are less conserved. A homology search of BcXYG1 in fungal genomes revealed the presence GH12 proteins of the first group in the genomes of all the necrotrophic and hemibiotrophic plant pathogenic fungi that were included in this search, namely *Colletotrichum gloeosporioides*, *Magnaporthe oryzae*, *Cochliobolus heterostrophus*, and *S. sclerotiorum* (Supplemental Fig. S2). However, we did not find class 1 GH12 proteins in the biotrophic pathogens that we examined, including *B. graminis* f. sp. *hordei*, *U. maydis*, and *Puccinia* spp., as well as in the human pathogen *C. albicans*. This finding suggests that BcXYG1 belongs to a specific subgroup of GH12 proteins, which may have evolved to facilitate the disease of fungal pathogens by inducing necrosis. Because early necrosis has a negative effect on the development of biotrophic pathogens, this class of proteins might have been removed from their genomes during evolution. In addition to the mentioned pathogens, we also found homologs of BcXYG1 in saprotrophic fungi that colonize and grow on dead plant residues. While these species probably do not need the necrosis-inducing activity during their life cycle, they may benefit from the xyloglucan-degrading endoglucanase activity of these proteins.

The specific induction of the *bcxyg1* gene in planta and the accumulation of high levels of the BcXYG1 protein during the early stage of infection connect BcXYG1 with in planta development and pathogenicity. Furthermore, we found homologs of BcXYG1 in necrotrophic and hemibiotrophic pathogens, which benefit from host cell death, but not in biotrophic pathogens, in which host cell death blocks infection. Despite this evidence, which supports a role of BcXYG1 in *B. cinerea* pathogenicity, we did not observe differences in lesion size produced by *B. cinerea* deletion mutants that lack BcXYG1 (Supplemental Fig. S7). This result is not surprising in light of the presence of additional NIPs in the fungal secretome. Indeed, similar results were reported in analyses of other *B. cinerea* NIPs, such as BcNEP1/2 (Cuesta Arenas et al., 2010) and BcIEB1 (Frías et al., 2016).

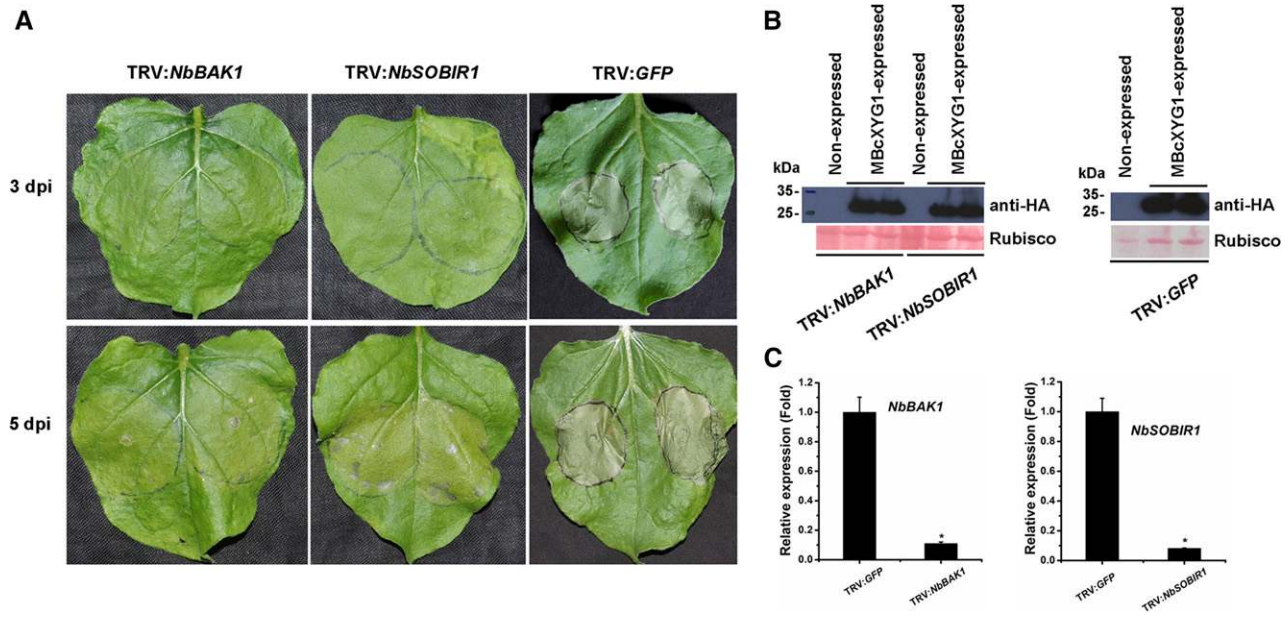

Figure 11. The necrosis-inducing activity of BcXYG1 is mediated by *NbBAK1* and *NbSOBIR1*. TRV-based VIGS vectors were used to initiate the silencing of *NbBAK1* (TRV:*NbBAK1*) and *NbSOBIR1* (TRV:*NbSOBIR1*). TRV:*GFP* was used as a control virus treatment in these experiments. A, Three weeks after the initiation of VIGS, *MBcXYG1* (+SP) was transiently expressed in the gene-silenced leaves using *A. tumefaciens* infiltration. Leaves were photographed 3 and 5 d after treatment. B, Immunoblot analysis of proteins from the indicated *N. benthamiana* leaves transiently expressing MBcXYG1-HA. Top gels, MBcXYG1-HA was detected using anti-HA antibodies; bottom gels, Ponceau S-stained blots showing the Rubisco large subunit. C, Tobacco *NbBAK1* and *NbSOBIR1* expression levels after VIGS treatment determined by qRT-PCR analysis. The expression level in control plants (TRV:*GFP*) was set as 1. *NbEF1α* was used as an endogenous control. Means and SD from three biological replicates are shown. Asterisks indicate significant differences ($P \leq 0.01$).

Our working model predicts that NIPs are necessary for the production of local necrosis during the early stage of infection. Accordingly, mutants in NIP-encoding genes are expected to be affected specifically in the production of early necrosis, but not at the stage of spreading lesion. To determine the possible effect of BcXYG1 in an early stage of the disease, we analyzed the infection of bean leaves using PathTrack, a noninvasive, automated system for live imaging and quantitative measurement of disease development (Eizner et al., 2017). This analysis revealed that the leaves infected with the *BcXYG1* overexpression strains OEXYG1 or OEMXYG1 produced earlier and more intense local necrosis. Importantly, the later lesion expansion rate was unchanged compared with the wild-type strain, which explains the similar lesion size at 72 hpi. This result shows the specific role of BcXYG1 in the generation of the early necrotic zone, which is necessary for initial disease establishment. Similarly, a NEP1 overexpression strain also showed earlier and more intense necrosis (Fig. 5), supporting the general role of NIPs in disease establishment. Previous analysis of *nep1* deletion strains revealed no change in pathogenicity of the mutants, precluding the determination of a role of this NIP in pathogenicity (Cuesta Arenas et al., 2010). Therefore, gain of function coupled with a more detailed analysis of pathogenicity (e.g. using PathTrack) can reveal hidden roles of previously unrecognized pathogenicity factors such as NIPs and other types of effectors.

Several studies have reported that necrotrophic fungi, such as *B. cinerea*, *S. sclerotiorum*, and *Plectosphaerella cucumerina*, might have a hemibiotrophic phase that precedes killing of the host cells (Williams et al., 2011; Kabbage et al., 2013, 2015; van Kan et al., 2014; Pétriacq et al., 2016). Indeed, necrotrophic pathogens such as *P. cucumerina* can shorten the biotrophic stage dependent on the spore densities at localized leaf areas during early infection, thereby gaining the advantage of immunity-related cell death in the host plant (Pétriacq et al., 2016). According to this new definition, the signal exchange and type of interactions during this short phase may determine the outcome of infection. We did not observe a hemibiotroph-like development in our experimental conditions; however, there is a very short time period that lasts about 24 h in which hyphae develop on the surface of the plant without the development of visible necrotic symptoms. This period is shortened in leaves infected by the BcXYG1- and MBcXYG1-expressing strains due to the earlier secretion of BcXYG1. Despite the earlier appearance of initial necrotic spots in the overexpression strain-infected leaves, disease progression was almost unaffected. A possible explanation for this result might be the activation of plant defense by BcXYG1, which counteracts the cell death-promoting activity. Accordingly, overexpression of *bcxyg1* not only stimulates the production of local necrosis but also causes earlier activation of the plant defense. In our interpretation, the short, symptomless phase, which has been referred to as

hemibiotrophic, is not synonym for a biotrophic phase but rather for a phase in which the fungus grows on the surface of the leaf, thus avoiding direct contact with the plant hostile environment while releasing factors such as BcXYG1 that cause necrosis underneath. These factors, at the same time, are recognized by the plant immune system, leading to defense activation. Hence, constitutive overexpression of NIPs may destroy the delicate balance between the fungus and host and may have negative effects on disease progression, despite earlier and increased levels of necrosis. This scenario is supported by results reported in the CA-BcRAC strain (Minz-Dub et al., 2013). This mutant shows earlier and markedly enhanced necrosis; however, lesion size at 72 hpi is slightly smaller than in wild-type infected leaves. Our current proteomic analysis showed high accumulation of several NIPs in secretome of the CA-BcRAC strain, including NPP1 (14.37-fold increase over the wild-type secretome) and BcSpl1 (1.64-fold increase). BcSpl1 contributes to the necrosis-inducing activity and the virulence of *B. cinerea*, but it also can induce systemic resistance of the host plant to pathogens (Frías et al., 2011, 2013).

The activation of defense by BcXYG1 probably involves signaling through the salicylic acid (SA) or jasmonic acid (JA)/ethylene (ET) signaling pathways. The SA signaling pathway is well known in the immune response against biotrophic pathogens, whereas the JA/ET pathway has been associated with defense against necrotrophs (Durrant and Dong, 2004; Glazebrook, 2005; Grant and Lamb, 2006). A previous study has demonstrated that *B. cinerea* manipulates the antagonistic effects between SA and JA immune pathways to enhance tomato susceptibility by secreting a β-(1,3)(1,6)-D-glucan, which can activate the SA signal pathway, which also inhibits JA signaling through NPR-1 (El Oirdi et al., 2011). However, many studies also have shown that cross talk between SA and JA/ET signaling pathways, either antagonistic and/or synergistic, can optimize the defense response against different classes of pathogens (Ferrari et al., 2003; Mur et al., 2006; Guo and Stotz, 2007; Spoel et al., 2007; Koornneef and Pieterse, 2008). We showed here that infiltration of leaves with BcXYG1 induces genes of both the SA and JA signal pathways, indicating that BcXYG1 triggers the host plant defense response through multisignal pathways. Similar results have demonstrated that several effectors and phytotoxin from *B. cinerea* and other pathogens can trigger both SA- and JA-mediated defense in plants (Rossi et al., 2011; Zhang et al., 2015, 2017; Xiang et al., 2017). However, which signal pathway is more significant and the exact relationships among these signal pathways remain largely unknown and require further investigation.

MATERIALS AND METHODS

Fungi, Bacteria, Plants, Growth Conditions, and Inoculation

Botrytis cinerea B05.10 wild-type strain and derived mutants were used in this study (for details, see Supplemental Table S5). All strains were routinely grown on PDA (Acumedia) and maintained at 22°C under continuous fluorescent light supplemented with near-UV (black) light. Conidia were obtained from 7-d-old cultures. *Escherichia coli* strains DH5α and Rosetta-gami (DE3) were used to propagate plasmids and express target proteins, respectively. *Agrobacterium tumefaciens* strain GV3101 was used for *A. tumefaciens*-mediated transient expression of proteins in plant leaves. Bean (*Phaseolus vulgaris* 'French bean', genotype N9059), tobacco (*Nicotiana benthamiana*), wheat (*Triticum aestivum*), and tomato (*Solanum lycopersicum*) plants were grown in a greenhouse (16-h/8-h intervals of 25°C/22°C, light/dark).

Pathogenicity assays of *B. cinerea* on bean were performed as described previously (Shlezinger et al., 2011). Conidia were collected from plates, washed, and suspended in inoculation medium (Gamborg's B5 medium supplemented with 2% (w/v) Glc and 10 mM KH_2PO_4/K_2HPO_4, pH 6.4). The primary leaves of 9-d-old bean were inoculated with 7.5-μL conidial suspensions (2×10^5 conidia mL^{-1}), the infected plants were incubated in a humid chamber at 22°C under fluorescent illumination for 72 h, and the lesion diameter was then measured. When specified, PathTrack (Eizner et al., 2017) was used to determine infection kinetics and parameters.

Preparation of the *B. cinerea* Secretome

Bean leaves were placed in glass trays with moist filter paper, and 50-mL droplets of conidia suspension (5×10^5 conidia mL^{-1}) were applied on 50 leaves so that they covered the entire leaf. Inoculated leaves were incubated in a humid chamber at 22°C for 28 h, and the inoculation suspension was then collected from the leaves, centrifuged at 4,000*g* for 10 min at 4°C, and the supernatant was collected into a fresh tube. The samples were filtered through a 0.45-μm Minisart nonpyrogenic filter (Sartorius-Stedim Biotech) to remove residual mycelia, conidia, and plant residues and then further purified using Amicon Ultra-4 Centrifugal Filter Devices (4 mL, 10 kD; Merck Millipore) to remove remnants of the inoculation medium and small toxins such as botrydial and other types of toxic molecules. The clean samples were dissolved in 4 mL of PBS and stored at –80°C. To test for necrosis-inducing activity, the clean secretome was infiltrated into *N. benthamiana* leaves using a syringe, and necrosis development was determined after 48 to 96 h. For the detection of proteins in the secretome, samples were separated by SDS gel electrophoresis and stained with silver reagent.

Proteomic Analysis

Sample Preparation

Purified secretome samples were frozen at −80°C and then lyophilized overnight using a Christ Delta 1-24 LSC Freeze Dryer lyophilizer (SciQuip). Dried proteins were resuspended in 8 M urea (Sigma) with 0.1 M Tris-HCl, pH 7.9, on ice for 10 min. Proteins were reduced by incubation with DTT (5 mM; Sigma) for 1 h at room temperature and alkylated with 10 mM iodoacetamide (Sigma) in the dark for 45 min. Samples were diluted to 2 M urea with 50 mM ammonium bicarbonate. Proteins were then subjected to digestion with trypsin (Promega) overnight at 37°C (50:1 protein amount:trypsin), followed by a second trypsin digestion for 4 h. The digestions were stopped by the addition of trifluroacetic acid (1%). Following digestion, peptides were desalted using solid-phase extraction columns (Oasis HLB; Waters). The samples were stored at −80°C until further analysis.

Liquid Chromatography

Ultra-performance liquid chromatography/mass spectrometry-grade solvents were used for all chromatographic steps. Each sample was loaded using a splitless nano-ultra-performance liquid chromatograph (10 kpsi nanoAcquity; Waters). The mobile phase was water + 0.1% formic acid (A) and acetonitrile + 0.1% formic acid (B). Desalting of the samples was performed online using a reverse-phase C18 trapping column (180 μm i.d., 20 mm length, 5 μm particle size; Waters). The peptides were then separated using a T3 HSS nano-column (75 μm i.d., 250 mm length, 1.8 μm particle size; Waters) at 0.35 μL min^{-1}. Peptides were eluted from the column into the mass spectrometer using the following gradient: 4% to 30% B in 105 min, 30% to 90% B in 5 min, maintained at 90% for 5 min, and then back to the initial conditions.

Mass Spectrometry and Data Acquisition

The nano-ultra-performance liquid chromatograph was coupled online through a nanoESI emitter (10 μm tip; New Objective) to a quadrupole orbitrap

mass spectrometer (Q Exactive Plus; Thermo Scientific) using a FlexIon nanospray apparatus (Proxeon). Data were acquired in DDA mode using a Top10 method. MS1 resolution was set to 70,000 (at 400 mass-to-charge ratio), and maximum injection time was set to 20 ms. MS2 resolution was set to 17,500, with maximum injection time of 60 ms.

Data Processing and Analysis

Raw data were imported into the Expressionist software (Gene Data) and processed as described previously (Shalit et al., 2015). The software was used for retention time alignment and peak detection of precursor peptides. A master peak list was generated from all tandem mass spectrometry events and sent for database search using Mascot version 2.5 (Matrix Sciences). The data were searched against a database containing protein sequences of *B. cinerea* downloaded from http://www.broadinstitute.org/annotation/genome/botrytis_cinerea/MultiDownloads.html (botrytis_cinerea__b05.10_vankan__1_proteins.fasta) as well as bean and Arabidopsis (*Arabidopsis thaliana*) protein sequences downloaded from UniProt. Fixed modification was set to carbamidomethylation of Cys, and variable modification was set to oxidation of Met. Search results were then filtered using the ProteinProphet algorithm (Nesvizhskii et al., 2003) to achieve a maximum false discovery rate of 1% at the protein level. Peptide identifications were imported back to Expressionist to annotate the identified peaks. Quantification of proteins from the peptide data was performed using an in-house script (Shalit et al., 2015). Data were normalized based on the total ion current. Protein abundance was calculated by summing the three most intense, unique peptides per protein. Student's *t* test, after logarithmic transformation, was used to identify significant differences across the biological replicates. Fold changes were calculated based on the ratio of arithmetic means of the case versus control samples.

Bioinformatics Analysis and Programs Used in This Study

The genomic sequence database of *B. cinerea* at JGI (http://genome.jgi.doe.gov/Botci1/Botci1.home.html) was used to characterize *B. cinerea* genes. The SignalP 4.1 server (http://www.cbs.dtu.dk/services/SignalP/) and SMART MODE (http://smart.embl-heidelberg.de/smart/change_mode.pl) were used to analyze the signal peptide sequence and protein domain. The National Center for Biotechnology Information (NCBI) and UniProt (http://www.uniprot.org/blast/) databases were used for BLASTp analysis. The ClustalW and Jalview programs were used for mature proteins alignments. The MEGA 5 program was used to generate the phylogenetic tree with an unrooted neighbor-joining method. PredictProtein (https://www.predictprotein.org/) was used to predict disulfide bonds in protein. ASA-View (http://www.abren.net/asaview/) was used to analyze the surface accessibility of proteins. The 3D structural models were predicted using I-TASSER (http://zhanglab.ccmb.med.umich.edu/I-TASSER/).

Extraction and Manipulation of DNA and RNA

Relative gene expression levels were determined by qRT-PCR as described previously (Zhu et al., 2013). For the measurement of *BcXYG1* gene expression during infection, bean leaves were sprayed with *B. cinerea* conidia (5×10^5 conidia mL^{-1}). Samples were obtained at 12, 24, 36, 48, 60, and 72 hpi, immediately frozen in liquid nitrogen, and stored at –80°C.

To compare *BcXYG1* transcript levels in different fungal strains, cultures were produced on PDA covered with cellophane, and the mycelia were collected after 3 d and stored at –80°C.

Genomic DNA of fungi was isolated using the NucleoSpin DNA kit (Macherey-Nagel) according to the manufacturer's instructions. Total plant and fungal RNA was isolated using the NucleoSpin RNA kit (Macherey-Nagel) according to the manufacturer's instructions and stored at –80°C. For cDNA synthesis, RNA samples were first treated with DNase I (Thermo Scientific), and the RevertAid First Strand cDNA Synthesis Kit (Thermo Scientific) was then used to generate the first-strand cDNA.

qRT-PCR was performed using the CFX96 Touch Real-Time PCR Detection System (Bio-Rad) and SYBR Premix Ex Taq II (Takara Biotechnology) according to each manufacturer's instructions. Primers were designed across or flanking an intron (Supplemental Table S6). The relative expression levels of the *B. cinerea* *Bcgpdh* gene (*BC1G_05277*) and the bean *Actin-11* gene (GenBank accession no. EH040443.1) were used as references for normalizing the RNA sample. For each examined gene, qRT-PCR assays were repeated at least twice, each repetition with three independent replicates.

Plasmid Construction

Oligonucleotides used for plasmid construction are described in Supplemental Table S6. The *BcXYG1* replacement construct was generated as described (Ma et al., 2017a). The 5′ (538 bp) and 3′ (534 bp) flanks of the *BcXYG1* open reading frame were amplified by PCR from genomic DNA of the wild-type strain B05.10, and the fragments were cloned into the upstream and downstream regions, respectively, of the *hph* cassette using the Gibson Assembly Master Mix kit (New England Biolabs). To construct the *BcXYG1* overexpression vector, the full-length *BcXYG1* open reading frame fused with an HA tag at the C terminus was cloned into the pH2G vector between the *B. cinerea* histone H2B promoter (NCBI identifier CP009806.1) and the endo-β-1,4-glucanase precursor terminator (NCBI identifier CP009807.1).

To construct the *E. coli* protein expression vectors, the sequence encoding mature BcXYG1 protein without the signal peptide was cloned into pET-22b (+) (Novagen) to generate the expression vector pET22b-BcXYG1-6×His. For transient expression of proteins in plants using the *A. tumefaciens* infiltration method, the sequence encoding Arabidopsis PR3 (TAIR identifier AT3G12500) signal peptide was fused upstream of the BcXYG1-HA fusion protein, and the construct was cloned into pCAMBIA3300 (Cambia) between the cauliflower mosaic virus 35S promoter and the NOS terminator. Expressions vectors of additional genes were similarly constructed.

Characterization of *B. cinerea* Transformants

Transformation of *B. cinerea* was performed as described previously (Ma et al., 2017a). The following transgenic strains were produced: Δ*xyg1* (deletion of *BcXYG1*), OEXYG1 (overexpression of an HA-tagged native form of *BcXYG1*), and OEMXYG1 (overexpression of an HA-tagged mutated form of *BcXYG1* that shows no enzymatic activity). Deletion of *BcXYG1* was confirmed by PCR using appropriate primers (Supplemental Table S6). Overexpression of *BcXYG1* was determined by qRT-PCR and using the *Bcgpdh* (*BC1G_05277*) gene to normalize the RNA sample. Two independent strains from *BcXYG1* deletion mutants (Δ*xyg1-1* and Δ*xyg1-2*) were selected for growth and development characterization. To assay growth rates, strains were cultured on PDA at 22°C for 2 d, and mycelial plugs were taken from the colony edge, placed in the center of a fresh PDA petri dish, and incubated at 22°C either in light (24 h of fluorescent light supplemented with near-UV light) or in complete darkness. Colony morphology and sclerotia formation were monitored after 7 and 15 d in light- and dark-incubated cultures, respectively. For the stress tolerance assay, examined strains were inoculated onto PDA plates containing 1 M NaCl, 1 M sorbitol, 0.3 mg mL^{-1} Calcofluor White, 0.5 mg mL^{-1} Congo Red, and 0.02% SDS, as described previously (Ma et al., 2017a).

Transient Expression, Protein Extraction, and Immunoblot Analysis

A. tumefaciens-mediated transient expression was performed using leaf infiltration, as described previously (Kettles et al., 2017). Proteins were extracted from *B. cinerea* and plants, and immunoblot analysis was performed as described (Wei et al., 2016). Briefly, approximately 0.2 g of tissue was ground to powder in liquid nitrogen and suspended in 1 mL of lysis buffer (50 mM Tris, pH 7.4, 150 mM NaCl, 1% Triton X-100, 1 mM EDTA, and 1 mM phenylmethylsulfonyl fluoride). Samples were incubated on ice for 5 min and then centrifuged at 13,200*g* for 10 min at 4°C to remove residues. The supernatant with the soluble proteins was mixed with 4× SDS sample buffer (40% glycerol, 240 mM Tris-HCl, pH 6.8, 8% SDS, 0.04% Bromophenol Blue, and 5% β-mercaptoethanol) and then denatured by boiling (100°C) for 5 min. Proteins were separated by SDS-PAGE and blotted onto membranes, and the blots were analyzed using anti-HA or anti-His antibodies (Sigma).

To confirm the secretion of the BcXYG1-HA and MBcXYG1-HA fusion proteins by the transgenic strains, mycelia were cultured in PDB for 3 d, and the medium was collected, filtered with a 0.45-μm Minisart nonpyrogenic filter (Sartorius-Stedim Biotech), frozen at –80°C, and dried overnight using a lyophilizer. The dry powder was dissolved in 250 μL of PBS and frozen at –80°C for further immunoblot analysis.

Expression, Purification, and Enzyme Activity Analysis of Recombinant BcXYG1 Protein

The *E. coli* strain Rosetta-gami (DE3) was used to express the recombinant proteins. Expression of the recombinant proteins in *E. coli* was performed according to the Novagen pET System Manual 11th Edition. Purification of recombinant proteins

was performed using Ni-NTA resin (GE Healthcare) as described (Zhang et al., 2015). Enzymatic activity of BcXYG1 and MBcXYG1 was determined at room temperature using xyloglucan as substrate in a final volume of 20 μL containing 50 mM ammonium acetate, pH 5, 50 μg of polysaccharide (xyloglucan from tamarind [*Tamarindus indica*], Rhamnogalacturonan I, or Rhamnogalacturonan II), and the examined protein. Following the enzymatic assays, the samples were dried by a SpeedVac, resuspended in 200 μL of distilled, deionized water, and again dried using a SpeedVac. Each dry sample was supplemented with 30 μL of distilled, deionized water, vortexed, and kept at 8°C until matrix-assisted laser-desorption ionization (MALDI) analysis. For the MALDI analysis, a 1-μL sample was spotted on the grid, while wet 1 μL of matrix was added and mixed. The matrix used was 1 μL of DHB in methanol. MALDI was carried out in the positive mode.

Protein Infiltration Assays and Induction of Plant Systemic Resistance by BcXYG1

To test the induction of plant necrosis by recombinant proteins produced in *E. coli*, BcXYG1 was dissolved in PBS and infiltrated into *N. benthamiana* leaves using a syringe. Plants were kept in a growth chamber at 25°C and photographed at 5 d post infection. Additional treatments included infiltration with 100 μg mL^{-1} MBcXYG1, EGFP, and BcXYG2.

To test for induced systemic defense responses in plants, one of two primary leaves of 9-d-old bean was infiltrated with 500 μL of 100 μg mL^{-1} examined protein. Treated plants were kept in a growth chamber for 2 d, and the second (untreated) leaf was then inoculated with *B. cinerea* conidia or was picked and stored at –80°C for RNA extraction and qRT-PCR analysis. Inoculated plants were incubated in a humid chamber at 22°C for an additional 72 h, and the lesions were then measured and photographed.

Protoplast Preparation and Assay

Tobacco protoplasts were prepared as described previously (Frías et al., 2014). To determine the possible toxicity of MBcXYG1, protoplasts were incubated with 100 μg mL^{-1} protein at 25°C with gentle agitation at 60 rpm. The number of intact and damaged protoplasts was determined using a light microscope at 0, 2, 4, 6, and 8 h following addition of the protein.

VIGS in *N. benthamiana*

VIGS was used to test the possible association of NbBAK1 and/or NbSOBIR1 with MBcXYG1-induced necrosis. *NbBAK1* or *NbSOBIR1* expression was silenced using VIGS, as described previously (Kettles et al., 2017). pTRV2-*GFP* was used as a control, and tobacco *NbBAK1* and *NbSOBIR1* expression levels were determined by qRT-PCR analysis as described previously (Franco-Orozco et al., 2017). Briefly, *A. tumefaciens* strain GV3101 harboring pTRV1, pTRV2-*GFP*, pTRV2-*NbBAK1*, or pTRV2-*NbSOBIR1* constructs were cultured in Luria-Bertani medium containing 50 μg mL^{-1} kanamycin and incubated at 28°C for 24 h. Bacteria cells were harvested by centrifugation at 5,000*g* and washed twice in infiltration buffer (10 mM $MgCl_2$ and 10 mM MES, pH 5.6), and cell density was adjusted to OD_{600} = 0.2. *A. tumefaciens* carrying either pTRV2-*NbBAK1* or pTRV2-*NbSOBIR1* was mixed at a 1:1 ratio with a strain carrying the pTRV1 plasmid. Acetosyringone (Sigma) was added to a final concentration of 200 μM, and the cultures were incubated at 28°C in the dark for 2 h and then infiltrated into *N. benthamiana* leaves using a 1-mL syringe. Virus-infected plants were maintained for 2 to 3 weeks in a growth chamber at 20°C, and the uninoculated upper leaves of the plants were then treated with MBcXYG1 (+SP) using the *A. tumefaciens*-mediated transient expression method. The plants were moved to a growth chamber at 25°C, and necrosis development was followed during the first 5 d after treatment.

Statistical Analysis

Statistical tests were performed using Origin 7.5 (OriginLab). Data significance was analyzed by ANOVA (one-way, $P \leq 0.01$). In all graphs, results represent mean values of three to five independent experiments ± SD. Different letters or asterisks in the graphs indicate statistical differences at $P \leq 0.01$.

Accession Numbers

Sequence data from this article can be found in the GenBank/EMBL data libraries under accession numbers. BcXYG1, BC1G_00594; BcXYG2, BC1G_01008; SS, XP_001598412.1; RN, GAP83653.1; PM, XP_007918908.1; CG, EQB54057.1; AO, XP_001820024.1; CH, XP_014075771.1; MO, XP_003717758.1; VD, XP_009654606.1; FG, XP_011324452.1; PS, XP_009525815.1; TR, XP_006967891.1; Pvd1, HM240258.1; PvPR1, CAA43637.1; PvPR2, CAA43636.1.

Supplemental Data

The following supplemental materials are available.

Supplemental Figure S1. Distribution of proteins found in the *B. cinerea* secretome.

Supplemental Figure S2. Sequence similarities between BcXYG1 and other GH12 proteins.

Supplemental Figure S3. Multiple sequence alignment of BcXYG2, which does not induce necrosis, BcXYG1, and other necrosis-inducing GH12 proteins.

Supplemental Figure S4. Enzymatic activity assay of BcXYG1 and MBcXYG1.

Supplemental Figure S5. *BcXYG1* gene deletion strategy and confirmation in *B. cinerea*.

Supplemental Figure S6. *bcxyg1* transgenic strains do not show developmental defects, and deletion of *bcxyg1* does not affect the induction of necrosis by the *B. cinerea* secretome.

Supplemental Figure S7. Virulence analysis of *B. cinerea* transgenic strains.

Supplemental Figure S8. Surface accessibility analysis of BcXYG1.

Supplemental Figure S9. Treatment with Dukatalon causes cell death but does not induce plant systemic resistance.

Supplemental Figure S10. Plant defense-stimulating activity of MBcXYG1 is dependent on its tertiary structure.

Supplemental Table S1. List of secreted proteins identified in the secretome of the *B. cinerea* wild-type strain.

Supplemental Table S2. Comparison of protein presence and abundance between mutant Δ*bcnoxA* and wild-type strains.

Supplemental Table S3. Comparison of protein presence and abundance between CA-BcRAC and wild-type strains.

Supplemental Table S4. List of priority category candidates that have been screened using *A. tumefaciens* infiltration assay of *N. benthamiana* leaves.

Supplemental Table S5. List of *B. cinerea* strains used in this study.

Supplemental Table S6. List of oligonucleotides used in this study.

ACKNOWLEDGMENTS

We thank Dr. Kostya Kanyuka at Rothamsted Research and Dr. Guido Sessa at Tel Aviv University for providing us the *A. tumefaciens* strains harboring the pTRV2-*NbBAK1*, pTRV2-*NbSOBIR1*, pTRV1, and pTRV2-*GFP* plasmids.

Received March 20, 2017; accepted July 11, 2017; published July 14, 2017.

LITERATURE CITED

Albert I, Böhm H, Albert M, Feiler CE, Imkampe J, Wallmeroth N, Brancato C, Raaymakers TM, Oome S, Zhang H, et al (2015) An RLP23-SOBIR1-BAK1 complex mediates NLP-triggered immunity. Nat Plants **1:** 15140

Benedetti M, Pontiggia D, Raggi S, Cheng Z, Scaloni F, Ferrari S, Ausubel FM, Cervone F, De Lorenzo G (2015) Plant immunity triggered by engineered in vivo release of oligogalacturonides, damage-associated molecular patterns. Proc Natl Acad Sci USA **112:** 5533–5538

Böhm H, Albert I, Oome S, Raaymakers TM, Van den Ackerveken G, Nürnberger T (2014) A conserved peptide pattern from a widespread microbial virulence factor triggers pattern-induced immunity in *Arabidopsis*. PLoS Pathog **10:** e1004491

Brito N, Espino JJ, González C (2006) The endo-beta-1,4-xylanase xyn11A is required for virulence in *Botrytis cinerea*. Mol Plant Microbe Interact **19:** 25–32

Cantarel BL, Coutinho PM, Rancurel C, Bernard T, Lombard V, Henrissat B (2009) The Carbohydrate-Active EnZymes database (CAZy): an expert resource for glycogenomics. Nucleic Acids Res **37:** D233–D238

Cuesta Arenas Y, Kalkman ERIC, Schouten A, Dieho M, Vredenbregt P, Uwumukiza B, Osés Ruiz M, van Kan JAL (2010) Functional analysis and mode of action of phytotoxic Nep1-like proteins of *Botrytis cinerea*. Physiol Mol Plant Pathol **74:** 376–386

De Wit PJ (2016) Apoplastic fungal effectors in historic perspective: a personal view. New Phytol **212:** 805–813

Du J, Verzaux E, Chaparro-Garcia A, Bijsterbosch G, Keizer LC, Zhou J, Liebrand TW, Xie C, Govers F, Robatzek S, et al (2015) Elicitin recognition confers enhanced resistance to *Phytophthora infestans* in potato. Nat Plants **1:** 15034

Du Y, Stegmann M, Misas Villamil JC (2016) The apoplast as battleground for plant-microbe interactions. New Phytol **209:** 34–38

Durrant WE, Dong X (2004) Systemic acquired resistance. Annu Rev Phytopathol **42:** 185–209

Eizner E, Ronen M, Gur Y, Gavish A, Zhu W, Sharon A (2017) Characterization of *Botrytis*-plant interactions using PathTrack©: an automated system for dynamic analysis of disease development. Mol Plant Pathol **18:** 503–512

El Oirdi M, El Rahman TA, Rigano L, El Hadrami A, Rodriguez MC, Daayf F, Vojnov A, Bouarab K (2011) *Botrytis cinerea* manipulates the antagonistic effects between immune pathways to promote disease development in tomato. Plant Cell **23:** 2405–2421

Espino JJ, Gutiérrez-Sánchez G, Brito N, Shah P, Orlando R, González C (2010) The *Botrytis cinerea* early secretome. Proteomics **10:** 3020–3034

Fang A, Han Y, Zhang N, Zhang M, Liu L, Li S, Lu F, Sun W (2016) Identification and characterization of plant cell death-inducing secreted proteins from *Ustilaginoidea virens*. Mol Plant Microbe Interact **29:** 405–416

Ferrari S, Plotnikova JM, De Lorenzo G, Ausubel FM (2003) Arabidopsis local resistance to *Botrytis cinerea* involves salicylic acid and camalexin and requires EDS4 and PAD2, but not SID2, EDS5 or PAD4. Plant J **35:** 193–205

Ferrari S, Savatin DV, Sicilia F, Gramegna G, Cervone F, Lorenzo GD (2013) Oligogalacturonides: plant damage-associated molecular patterns and regulators of growth and development. Front Plant Sci **4:** 49

Franco-Orozco B, Berepiki A, Ruiz O, Gamble L, Griffe LL, Wang S, Birch PRJ, Kanyuka K, Avrova A (2017) A new proteinaceous pathogen-associated molecular pattern (PAMP) identified in Ascomycete fungi induces cell death in Solanaceae. New Phytol **214:** 1657–1672

Frías M, Brito N, González C (2013) The *Botrytis cinerea* cerato-platanin BcSpl1 is a potent inducer of systemic acquired resistance (SAR) in tobacco and generates a wave of salicylic acid expanding from the site of application. Mol Plant Pathol **14:** 191–196

Frías M, Brito N, González M, González C (2014) The phytotoxic activity of the cerato-platanin BcSpl1 resides in a two-peptide motif on the protein surface. Mol Plant Pathol **15:** 342–351

Frías M, González C, Brito N (2011) BcSpl1, a cerato-platanin family protein, contributes to *Botrytis cinerea* virulence and elicits the hypersensitive response in the host. New Phytol **192:** 483–495

Frías M, González M, González C, Brito N (2016) BcIEB1, a *Botrytis cinerea* secreted protein, elicits a defense response in plants. Plant Sci **250:** 115–124

Furman-Matarasso N, Cohen E, Du Q, Chejanovsky N, Hanania U, Avni A (1999) A point mutation in the ethylene-inducing xylanase elicitor inhibits the beta-1-4-endoxylanase activity but not the elicitation activity. Plant Physiol **121:** 345–351

Gao Y, Faris JD, Liu Z, Kim YM, Syme RA, Oliver RP, Xu SS, Friesen TL (2015) Identification and characterization of the SnTox6-*Snn6* interaction in the *Parastagonospora nodorum*-wheat pathosystem. Mol Plant Microbe Interact **28:** 615–625

Glazebrook J (2005) Contrasting mechanisms of defense against biotrophic and necrotrophic pathogens. Annu Rev Phytopathol **43:** 205–227

González C, Brito N, Sharon A (2016) Botrytis: The Fungus, The Pathogen and Its Management in Agricultural Systems. Springer International Publishing, Switzerland, pp 229–246

Grant M, Lamb C (2006) Systemic immunity. Curr Opin Plant Biol **9:** 414–420

Guo X, Stotz HU (2007) Defense against *Sclerotinia sclerotiorum* in Arabidopsis is dependent on jasmonic acid, salicylic acid, and ethylene signaling. Mol Plant Microbe Interact **20:** 1384–1395

Kabbage M, Williams B, Dickman MB (2013) Cell death control: the interplay of apoptosis and autophagy in the pathogenicity of *Sclerotinia sclerotiorum*. PLoS Pathog **9:** e1003287

Kabbage M, Yarden O, Dickman MB (2015) Pathogenic attributes of *Sclerotinia sclerotiorum*: switching from a biotrophic to necrotrophic lifestyle. Plant Sci **233:** 53–60

Kettles GJ, Bayon C, Canning G, Rudd JJ, Kanyuka K (2017) Apoplastic recognition of multiple candidate effectors from the wheat pathogen *Zymoseptoria tritici* in the nonhost plant *Nicotiana benthamiana*. New Phytol **213:** 338–350

Koornneef A, Pieterse CMJ (2008) Cross talk in defense signaling. Plant Physiol **146:** 839–844

Kubicek CP, Starr TL, Glass NL (2014) Plant cell wall-degrading enzymes and their secretion in plant-pathogenic fungi. Annu Rev Phytopathol **52:** 427–451

Liebrand TW, van den Berg GC, Zhang Z, Smit P, Cordewener JH, America AHP, Sklenar J, Jones AM, Tameling WI, Robatzek S, et al (2013) Receptor-like kinase SOBIR1/EVR interacts with receptor-like proteins in plant immunity against fungal infection. Proc Natl Acad Sci USA **110:** 10010–10015

Lorang J, Kidarsa T, Bradford CS, Gilbert B, Curtis M, Tzeng SC, Maier CS, Wolpert TJ (2012) Tricking the guard: exploiting plant defense for disease susceptibility. Science **338:** 659–662

Lorang JM, Sweat TA, Wolpert TJ (2007) Plant disease susceptibility conferred by a "resistance" gene. Proc Natl Acad Sci USA **104:** 14861–14866

Ma L, Salas O, Bowler K, Oren-Young L, Bar-Peled M, Sharon A (2017a) Genetic alteration of UDP-rhamnose metabolism in Botrytis cinerea leads to the accumulation of UDP-KDG that adversely affects development and pathogenicity. Mol Plant Pathol **18:** 263–275

Ma Z, Song T, Zhu L, Ye W, Wang Y, Shao Y, Dong S, Zhang Z, Dou D, Zheng X, et al (2015) A *Phytophthora sojae* glycoside hydrolase 12 protein is a major virulence factor during soybean infection and is recognized as a PAMP. Plant Cell **27:** 2057–2072

Ma Z, Zhu L, Song T, Wang Y, Zhang Q, Xia Y, Qiu M, Lin Y, Li H, Kong L, et al (2017b) A paralogous decoy protects *Phytophthora sojae* apoplastic effector PsXEG1 from a host inhibitor. Science **355:** 710–714

Marianayagam NJ, Sunde M, Matthews JM (2004) The power of two: protein dimerization in biology. Trends Biochem Sci **29:** 618–625

Minz-Dub A, Kokkelink L, Tudzynski B, Tudzynski P, Sharon A (2013) Involvement of *Botrytis cinerea* small GTPases BcRAS1 and BcRAC in differentiation, virulence, and the cell cycle. Eukaryot Cell **12:** 1609–1618

Mur LAJ, Kenton P, Atzorn R, Miersch O, Wasternack C (2006) The outcomes of concentration-specific interactions between salicylate and jasmonate signaling include synergy, antagonism, and oxidative stress leading to cell death. Plant Physiol **140:** 249–262

Nesvizhskii AI, Keller A, Kolker E, Aebersold R (2003) A statistical model for identifying proteins by tandem mass spectrometry. Anal Chem **75:** 4646–4658

Noda J, Brito N, González C (2010) The *Botrytis cinerea* xylanase Xyn11A contributes to virulence with its necrotizing activity, not with its catalytic activity. BMC Plant Biol **10:** 38

Oliver RP, Friesen TL, Faris JD, Solomon PS (2012) *Stagonospora nodorum*: from pathology to genomics and host resistance. Annu Rev Phytopathol **50:** 23–43

Oliver RP, Solomon PS (2010) New developments in pathogenicity and virulence of necrotrophs. Curr Opin Plant Biol **13:** 415–419

Oome S, Raaymakers TM, Cabral A, Samwel S, Böhm H, Albert I, Nürnberger T, Van den Ackerveken G (2014) Nep1-like proteins from three kingdoms of life act as a microbe-associated molecular pattern in *Arabidopsis*. Proc Natl Acad Sci USA **111:** 16955–16960

Ottmann C, Luberacki B, Küfner I, Koch W, Brunner F, Weyand M, Mattinen L, Pirhonen M, Anderluh G, Seitz HU, et al (2009) A common toxin fold mediates microbial attack and plant defense. Proc Natl Acad Sci USA **106:** 10359–10364

Pétriacq P, Stassen JH, Ton J (2016) Spore density determines infection strategy by the plant pathogenic fungus *Plectosphaerella cucumerina*. Plant Physiol **170:** 2325–2339

Poinssot B, Vandelle E, Bentéjac M, Adrian M, Levis C, Brygoo Y, Garin J, Sicilia F, Coutos-Thévenot P, Pugin A (2003) The endopolygalacturonase 1 from Botrytis cinerea activates grapevine defense reactions unrelated to its enzymatic activity. Mol Plant Microbe Interact **16:** 553–564

Postma J, Liebrand TWH, Bi G, Evrard A, Bye RR, Mbengue M, Kuhn H, Joosten MHAJ, Robatzek S (2016) Avr4 promotes Cf-4 receptor-like protein association with the BAK1/SERK3 receptor-like kinase to initiate receptor endocytosis and plant immunity. New Phytol **210:** 627–642

Rossi FR, Gárriz A, Marina M, Romero FM, Gonzalez ME, Collado IG, Pieckenstain FL (2011) The sesquiterpene botrydial produced by *Botrytis cinerea* induces the hypersensitive response on plant tissues and its action is modulated by salicylic acid and jasmonic acid signaling. Mol Plant Microbe Interact **24:** 888–896

Sandgren M, Ståhlberg J, Mitchinson C (2005) Structural and biochemical studies of GH family 12 cellulases: improved thermal stability, and ligand complexes. Prog Biophys Mol Biol **89:** 246–291

Segmüller N, Kokkelink L, Giesbert S, Odinius D, van Kan J, Tudzynski P (2008) NADPH oxidases are involved in differentiation and pathogenicity in *Botrytis cinerea*. Mol Plant Microbe Interact **21:** 808–819

Sevier CS, Kaiser CA (2002) Formation and transfer of disulphide bonds in living cells. Nat Rev Mol Cell Biol **3:** 836–847

Shalit T, Elinger D, Savidor A, Gabashvili A, Levin Y (2015) MS1-based label-free proteomics using a quadrupole orbitrap mass spectrometer. J Proteome Res **14:** 1979–1986

Shi G, Friesen TL, Saini J, Xu SS, Rasmussen JB, Faris JD (2015) The wheat *Snn7* gene confers susceptibility on recognition of the *Parastagonospora nodorum* necrotrophic effector SnTox7. Plant Genome **8:** 1–10

Shlezinger N, Minz A, Gur Y, Hatam I, Dagdas YF, Talbot NJ, Sharon A (2011) Anti-apoptotic machinery protects the necrotrophic fungus *Botrytis cinerea* from host-induced apoptotic-like cell death during plant infection. PLoS Pathog **7:** e1002185

Spoel SH, Johnson JS, Dong X (2007) Regulation of tradeoffs between plant defenses against pathogens with different lifestyles. Proc Natl Acad Sci USA **104:** 18842–18847

Trouvelot S, Héloir MC, Poinssot B, Gauthier A, Paris F, Guillier C, Combier M, Trdá L, Daire X, Adrian M (2014) Carbohydrates in plant immunity and plant protection: roles and potential application as foliar sprays. Front Plant Sci **5:** 592

van Kan JAL, Shaw MW, Grant-Downton RT (2014) *Botrytis* species: relentless necrotrophic thugs or endophytes gone rogue? Mol Plant Pathol **15:** 957–961

Wei W, Zhu W, Cheng J, Xie J, Jiang D, Li G, Chen W, Fu Y (2016) Nox complex signal and MAPK cascade pathway are cross-linked and essential for pathogenicity and conidiation of mycoparasite *Coniothyrium minitans*. Sci Rep **6:** 24325

Williams B, Kabbage M, Kim HJ, Britt R, Dickman MB (2011) Tipping the balance: *Sclerotinia sclerotiorum* secreted oxalic acid suppresses host defenses by manipulating the host redox environment. PLoS Pathog **7:** e1002107

Williamson B, Tudzynski B, Tudzynski P, van Kan JA (2007) *Botrytis cinerea*: the cause of grey mould disease. Mol Plant Pathol **8:** 561–580

Wu J, Wang Y, Park SY, Kim SG, Yoo JS, Park S, Gupta R, Kang KY, Kim ST (2016) Secreted alpha-N-arabinofuranosidase B protein is required for the full virulence of *Magnaporthe oryzae* and triggers host defences. PLoS ONE **11:** e0165149

Xiang J, Li X, Yin L, Liu Y, Zhang Y, Qu J, Lu J (2017) A candidate RxLR effector from *Plasmopara viticola* can elicit immune responses in *Nicotiana benthamiana*. BMC Plant Biol **17:** 75

Zhang H, Wu Q, Cao S, Zhao T, Chen L, Zhuang P, Zhou X, Gao Z (2014a) A novel protein elicitor (SsCut) from *Sclerotinia sclerotiorum* induces multiple defense responses in plants. Plant Mol Biol **86:** 495–511

Zhang L, Kars I, Essenstam B, Liebrand TW, Wagemakers L, Elberse J, Tagkalaki P, Tjoitang D, van den Ackerveken G, van Kan JA (2014b) Fungal endopolygalacturonases are recognized as microbe-associated molecular patterns by the Arabidopsis receptor-like protein RESPONSIVENESS TO BOTRYTIS POLYGALACTURONASES1. Plant Physiol **164:** 352–364

Zhang L, Ni H, Du X, Wang S, Ma XW, Nürnberger T, Guo HS, Hua C (2017) The *Verticillium*-specific protein VdSCP7 localizes to the plant nucleus and modulates immunity to fungal infections. New Phytol **215:** 368–381

Zhang W, Fraiture M, Kolb D, Löffelhardt B, Desaki Y, Boutrot FF, Tör M, Zipfel C, Gust AA, Brunner F (2013) *Arabidopsis* receptor-like protein30 and receptor-like kinase suppressor of BIR1-1/EVERSHED mediate innate immunity to necrotrophic fungi. Plant Cell **25:** 4227–4241

Zhang Y, Zhang Y, Qiu D, Zeng H, Guo L, Yang X (2015) BcGs1, a glycoprotein from *Botrytis cinerea*, elicits defence response and improves disease resistance in host plants. Biochem Biophys Res Commun **457:** 627–634

Zhu W, Wei W, Fu Y, Cheng J, Xie J, Li G, Yi X, Kang Z, Dickman MB, Jiang D (2013) A secretory protein of necrotrophic fungus *Sclerotinia sclerotiorum* that suppresses host resistance. PLoS ONE **8:** e53901